Transportation Research Part B 155 (2022) 72–100

Contents lists available at ScienceDirect

Transportation Research Part B

journal homepage: www.elsevier.com/locate/trb

One-to-many matching and section-based formulation of autonomous ridesharing equilibrium

Mohamadhossein Noruzoliaee [a], Bo Zou [b,*]

[a] Department of Civil Engineering, University of Texas Rio Grande Valley, USA
[b] Department of Civil and Materials Engineering, University of Illinois at Chicago, USA

ARTICLE INFO

Keywords:
Shared autonomous vehicle
One-to-many matching
Section-based ridesharing equilibrium
Endogenous market share
Network congestion

ABSTRACT

This paper models autonomous ridesharing — multiple travelers simultaneously riding one shared autonomous vehicle (SAV) — in a network equilibrium setting with mixed SAV and human-driven vehicle (HV) traffic. We make two major methodological contributions. First, a novel *one (SAV)-to-many (riders) matching* is proposed to characterize the waiting times of an SAV and multiple travelers who share rides in the SAV during online matching, which is a nontrivial generalization of the one-to-one matching without ridesharing. Our matching characterization considers the possibilities of a traveler matched with an SAV starting from the same origin, whereto the SAV moved unoccupied as a result of either pickup or relocation, or with an in-service SAV that goes through the traveler's origin. Second, a *section-based formulation for SAV ridesharing user equilibrium* is introduced to characterize the SAV traveler flow, which accommodates the possibility that an SAV traveler's itinerary (OD pair) is different from that of the serving SAV and other travelers in the SAV. Unlike the existing link and route based ridesharing formulations, the notion of section both prevents undesired traveler en-route transfer(s) and allows travelers of multiple ODs to share rides, meanwhile respecting the SAV seat capacity constraint. In addition to the above two methodological contributions, the optimal *SAV fleet size, fare, routing, and allocation* (to in-service, pickup, and relocation states) decisions of a transportation network company (TNC) are formulated. The TNC decisions anticipate traveler reactions as characterized by a new multimodal autonomous ridesharing user equilibrium (MARUE), which is put forward with a proof of its existence and finds the endogenous market shares and road congestion effects of SAV/HV. Original insights are obtained from model implementation, including substantial systemwide benefit of ridesharing, marginal benefit of relocation in the presence of ridesharing, and diminishing economies of SAV size.

1. Introduction

Shared autonomous vehicles (SAVs) facilitate *ridesharing — multiple travelers sharing one vehicle at the same time* — which may reduce vehicle-miles traveled (VMT) given the travel demand due to efficient vehicle capacity utilization. To assess, this paper makes a first attempt in the literature to model autonomous ridesharing with SAVs in a multimodal network equilibrium setting with coexisting SAVs and human-driven vehicles (HVs). Two major methodological contributions are made. First, we propose a novel *one (SAV)-to-*

* Corresponding author.
E-mail addresses: h.noruzoliaee@utrgv.edu (M. Noruzoliaee), bzou@uic.edu (B. Zou).

https://doi.org/10.1016/j.trb.2021.11.002
Received 3 July 2020; Received in revised form 6 September 2021; Accepted 8 November 2021
Available online 27 November 2021

Nomenclature

Sets

M	vehicle types $m \in M =$ {shared autonomous vehicle (SAV), human-driven vehicle (HV)}
S	SAV movement states $s \in S = \{I, II, III\}$. *I*: in-service, *II*: pickup, and *III*: relocation
N	nodes of road network $n \in N$
A	links of road network $a \in A$
Z	zones $i \in Z \subseteq N$
R	routes (including one intra-zone route for each zone) $r \in R$
L	sections $l \in L$

Endogenous variables related to TNC decisions

F	SAV fleet size (number of SAVs)
f_d, f_0	SAV fare rates: distanced-based part ($/mi) and constant part ($/ride)
y_r^s	SAV flow on route r in movement state s (veh/hr)

Endogenous variables related to traveler flows

Q_{ij}^m	travel demand of vehicle type m for OD pair (i, j) (travelers/hr)
q_l	SAV traveler flow of section l (travelers/hr)
$\widetilde{q}_l$	a portion of SAV traveler flow of competing sections of section l and using routes that traverse l (travelers/hr)
q_{lr}	SAV traveler flow of section l and using SAV route r (travelers/hr)
x_{ai}	HV traveler flow on link a and destined to zone i (veh/hr)

Key endogenous variables related to matching and waiting

g_{ri}	variable indicating the possibility that travelers waiting in zone i can be picked up by in-service SAVs on route r which goes through i
$\mathscr{m}_i$	matching rate of zone i (matched SAV traveler groups/hr or matched SAVs/hr)
σ_i^q	search intensity of a traveler group in zone i
σ_i^y	search intensity of an SAV in zone i
ω_i^q	waiting time (due to matching) of an SAV traveler group originating from zone i (hr)
ω_i^y	waiting time (due to matching) of an SAV in matching with travelers who originate from zone i (hr)
ϖ_i	average waiting time (due to matching and meeting) of an SAV traveler originating from zone i (hr)
η_l	extra waiting time for SAV travelers of section l due to limited SAV seat capacity on the section (hr)
$\widetilde{\eta}_l$	extra waiting time for SAV travelers of section l due to limited SAV seat capacity on the competing sections (hr)

Key endogenous cost- and time-related variables

h_l	generalized cost of an SAV traveler on section l ($)
H_{ij}	minimum generalized travel cost of an SAV traveler for OD (i, j) ($)
c_a	generalized cost of an HV traveler on link a ($)
C_{ni}	minimum generalized travel cost of an HV traveler from node n to zone i ($)
t_a	vehicle travel time on link a (hr)
PT_i	parking search time in zone i (hr)
PC_i^m	operating cost of vehicle type m during parking search in zone i ($)

Key parameters and network correspondence indicators

Q_{ij}	total travel demand between OD pair (i, j) (travelers/hour)
κ	SAV (body) size, i.e., number of seats in an SAV
λ_{lr}	section-route correspondence indicator (=1 if route r traverses section l; =0 otherwise)
$\chi_{ll'}$	competing section indicator (=1 if section l' is a competing section of section $l \backslash l'$; =0 otherwise)
ϵ_{li}	section-zone correspondence indicator (=1 if zone i is an intermediate zone on section l; =0 otherwise)
ζ_{ri}	route-zone correspondence indicator (=1 if zone i is an intermediate zone on route r; =0 otherwise)
δ_{ar}	link-route correspondence indicator (=1 if link a lies on route r; =0 otherwise)
δ_{ar}^i	link-route-zone correspondence indicator (=1 if: 1) link a lies on route r; 2) zone i lies on route r; 3) the end of link a is no later than i on route r; =0 otherwise)

many (riders) matching characterization of the waiting times of an SAV and multiple travelers who share rides in the SAV while being matched via an online platform. In the relevant literature of ridesharing network equilibrium with HVs, waiting times of vehicles and riders due to matching are overlooked (Table 1). By introducing the notion of search intensity, the proposed one-to-many matching generalizes the one-to-one matching in non-shared ridehailing (e.g., Yang et al., 2010; Zha et al., 2016; Ban et al., 2019) which ends when a vehicle is matched with one traveler. The generalization is nontrivial due to the nonlinearity of SAV/traveler waiting times in

Table 1
Synthesis of existing network equilibrium studies of ridesharing and the present paper.

	Distributed ridesharing with HVs								Centralized ridesharing with SAVs
Author (year)/Model capability	Xu et al. (2015a)	Xu et al. (2015b)	Di et al. (2017)	Di et al. (2018)	Di and Ban (2019)	Li et al. (2020a)	Ma et al. (2020)	Chen and Di (2021)	This paper
Considers vehicle/rider wait times in one-to-many matching								✓**	✓
Prevents rider en-route transfer(s)	NR*		NR*			✓	NR*		✓
Allows riders of different ODs to share ride	NR*	✓	NR*	✓	✓		NR*	✓	✓
Considers vehicle relocation									✓

* NR means "not relevant", as the indicated studies considered the same OD for a vehicle and riders in the vehicle.
** The one-to-many matching function was used in Chen and Di (2021), which, as acknowledged by the authors, was borrowed from an earlier version of this paper (Noruzoliaee, 2018).

the number of travelers sharing rides in an SAV, which needs to respect the number of available seats in an SAV and be endogenously determined. Theoretical insights are derived by comparing the waiting times of an SAV/traveler due to matching with and without ridesharing.

In characterizing one-to-many matching, our contribution also includes comprehensive considerations of traveler-SAV matching possibilities with respect to the SAV movement states. Specifically, a traveler can be matched with an SAV which has the same origin as the traveler, or with an *in-service* SAV that goes through the traveler's origin and does not incur stopping other than picking up the traveler. For travelers matched with an SAV which has the same origin, we derive the total waiting time of these travelers due to matching and subsequently meeting the matched SAV. In doing so, our derivation recognizes the fact that SAVs starting from an origin consist of those moving to the origin as the result of either *pickup* — which starts once matching ends — or (proactive) *relocation* — which starts before matching ends based on anticipated demand. These two types of SAV movement states impose different total waiting times to travelers. For travelers matched with "going-through" SAVs in the in-service state, the total waiting time due to matching and waiting for the matched SAV is also derived.

The second major methodological contribution is the introduction of a *section-based formulation for SAV ridesharing user equilibrium*. Given that SAV ridesharing considered in the paper is comprehensive to allow: 1) an SAV and travelers in the SAV to have different origin-destination (OD) pairs, and 2) different travelers in an SAV to have different ODs, modeling the utilization of SAV seat capacity by travelers on and off an SAV is critical yet challenging. This issue similarly arises in ridesharing network equilibrium with HVs, but in our view has not been satisfactorily addressed (Table 1). Specifically, the literature of ridesharing network equilibrium with HVs has link- and route-based characterizations of traveler flow, vehicle flow, and traveler-vehicle mapping. Under the link-based formulation (Xu et al., 2015b; Di et al., 2018; Di and Ban 2019), it is possible to have a rider dropped off from a vehicle on the way (at the end of a link) and picked up by another vehicle (at the beginning of the next link) to complete the trip. Such *en-route transfer(s)* would be undesirable for riders and is not commonly seen in practice. The route-based formulation (Li et al. 2020a) prevents en-route transfer(s), but *does not allow travelers of different ODs to share rides at the same time*. More exactly, the route-based formulation allows a vehicle to serve multiple travelers who have different ODs along the vehicle route, but travelers on each link traversed by the vehicle route should have the same OD. This leads to an underutilization of vehicle seat capacity along a vehicle route.

The proposed section-based formulation both prevents rider en-route transfer(s) and allows travelers of different ODs to share rides at the same time, meanwhile respecting the SAV seat capacity constraint. Specifically, the notion of section is introduced to represent SAV traveler flows, in connection with routes on which SAV flows are modeled. We define a section as a sequence of zones connecting a traveler OD and traversed by at least one SAV route. Following this definition, multiple sections can be traversed by a common SAV route and thus compete for available seats of SAVs on the route. The utilization of SAV seat capacity is characterized at the section level, considering travelers of the section under study and of its competing sections. By doing so, the section-based formulation further allows for capturing additional waiting time of travelers of a section due to limited available SAV seats on the section.

Building on the proposed SAV ridesharing formulation, we put forward a new *multimodal autonomous ridesharing user equilibrium (MARUE)* and provide a proof for its existence. MARUE characterizes vehicle type choice, composed of three integrated parts. First is an autonomous ridesharing user equilibrium (ARUE), which assigns travelers to SAVs using a section-based representation of the SAV traveler network. ARUE explicitly accounts for one-to-many matching and SAV seat capacity constraint on each section. Second, a link-node based user equilibrium (UE) for loading HVs to road network is formulated, which also considers the congestion effect of SAVs. Lastly, ARUE and UE are integrated with endogenous SAV and HV market shares, which advances previous research that only distinguished between market shares of privately-owned autonomous vehicles and HVs (Chen et al. 2016a; van den Berg and Verhoef 2016; Noruzoliaee et al., 2018). MARUE further accounts for increased road capacity as SAVs can move closer together than HVs (Levin and Boyles 2015; Talebpour and Mahmassani 2016), and in-vehicle value of time (VOT) saving of SAV travelers as they can perform more desired activities than driving (Steck et al., 2018; Nazari et al., 2018). We formulate MARUE as nonlinear

complementarity and variational inequality problems, and develop its equivalent nonlinear program using a primal-dual gap function.

In addition to the above two major methodological contributions, in this paper we also seek the optimal supply decisions of SAVs, assumed to be made by a transportation network company (TNC) and including *SAV fleet size, fare, routing, and allocation* (to the in-service, pickup, and relocation states). Different from conventional ridesharing with HVs, where a TNC acts as a matching agency that pairs riders with HVs that are operated/owned by human drivers, autonomous ridesharing with SAVs enables central routing and allocation operations, fleet ownership, and lower service pricing due to absence of human drivers. The TNC decisions are modeled as a Stackelberg game. Given the SAV purchase price, the profit-maximizing TNC makes its SAV supply decisions, anticipating the travelers' reactions as characterized by MARUE and the road congestion. The overall TNC-traveler problem is formulated as a mathematical program with complementarity constraints (MPCC) and solved using the active set algorithm (Lawphongpanich and Yin 2010).

Overall, this paper makes a helpful contribution to the growing efforts of modeling SAV operations, which so far has relied only on optimization methods (Liang et al., 2016; Ma et al., 2017; Levin 2017; Hyland and Mahmassani 2018) or simulation techniques (Fagnant and Kockelman 2014; Fagnant et al., 2015; Chen et al. 2016b; Chen and Kockelman 2016; Azevedo et al., 2016; Boesch et al., 2016). To our knowledge, SAV ridesharing was considered in only a few simulation studies (Farhan and Chen 2018; Levin et al., 2017; Fagnant and Kockelman 2018). While valuable insights were offered, existing simulation studies have not provided answers to two key questions: 1) the optimal supply (fleet size, fare, and vehicle routing and allocation) of a centralized SAV service while competing with HVs, and 2) the equilibrium state of the transportation system that simultaneously allows for autonomous ridesharing and conventional driving.

Several original insights are obtained from numerical implementation of the model. First, we find that SAV ridesharing brings substantial benefits to the system performance (in terms of reduced total and occupied VMT, total travel time, and total travel cost), travelers (in terms of smaller wait time in matching), and the TNC (in terms of increased TNC profit) compared to a system in which ridesharing is not allowed in using SAVs. Second, SAV relocation brings only marginal benefits to the overall transportation system compared to a system in which vacant SAVs cannot proactively relocate. Third, the transportation system will benefit from increasing SAV size (number of SAV seats), but the marginal effect is diminishing. These insights, which are first-of-its-kind in a mixed environment with SAV/HV, advance the understanding of how transportation system performance can be reshaped by SAV ridesharing.

The rest of the paper is organized as follows. Section 2 presents the network representation in which the notion of section is introduced to capture different routings of SAVs and SAV travelers due to ridesharing. Section 3 conceptually describes the problem, including the TNC and traveler decision-making, based on which ARUE is defined. Section 2 and 3 are intended to help readers have an overall picture while navigating the mathematical modeling details presented in Sections 4 and 5. Section 4 presents the formulation of MARUE, based on which the TNC's decision problem is formulated in Section 5. The solution method is discussed in Section 6, followed by numerical analyses in Section 7. The paper concludes in Section 8.

2. Network representation

This section introduces a network representation to characterize the *vehicle* and *traveler* flows of SAVs and HVs. We consider an urban area which is divided into zones $i \in Z$ that generate/attract travel demand. Travel demand from zone i to zone j, referred to as OD (i, j), is denoted by Q_{ij}. The area has a road network which is characterized by a directed graph $G(N, A)$ comprising nodes $n \in N$ and links $a \in A$. The nodes represent intersections and links represent roads. A subset of nodes also acts as zones. Non-zone nodes, while not

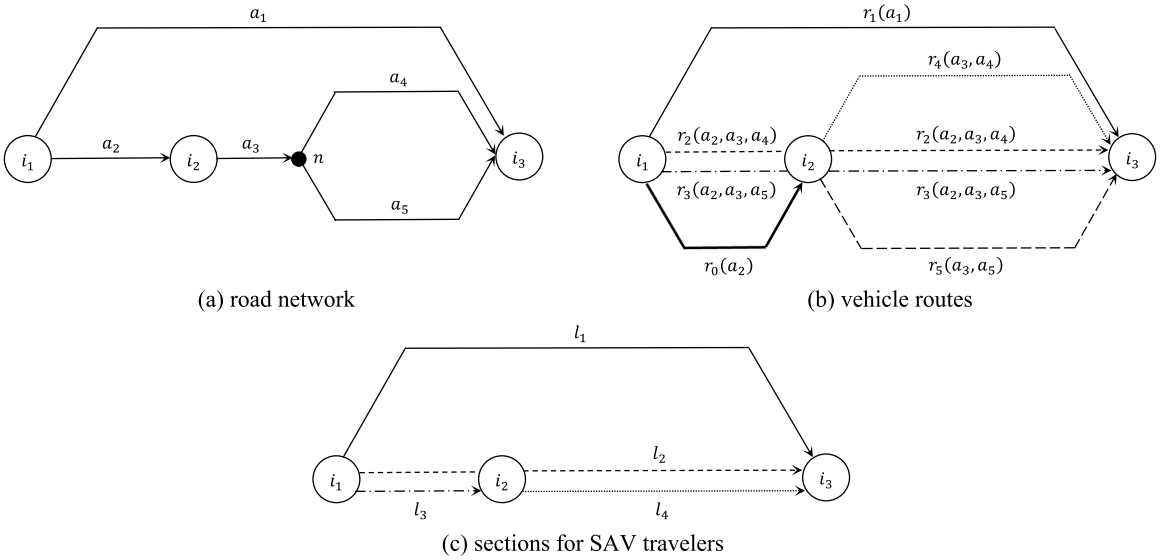

Fig. 1. Representations of: (a) road network, (b) vehicle routes, and (c) sections for SAV travelers.

generating/attracting travel demand, are necessary for characterizing links, as a link may have either one or both ends being non-zone nodes. Links are the basic elements on which vehicle (both SAVs and HVs) travel time is calculated.

The vehicle flows of SAVs and HVs between each OD *(i, j)* are characterized by a set of vehicle routes R_{ij}, each of which is assumed an acyclic sequence of links starting from zone *i* and ending in zone *j*. To illustrate, the road network in Fig. 1(a) has four nodes i_1, i_2, i_3, and *n*. i_1, i_2, and i_3 also act as zones and *n* is a non-zone node. We consider three ODs: (i_1,i_2), (i_1,i_3), and (i_2,i_3). Fig. 1(b) shows the routes for each of the three ODs. For example, OD (i_1,i_3) has three routes: $r_1(a_1)$, $r_2(a_2,a_3,a_4)$ and $r_3(a_2,a_3,a_5)$. $r_1(a_1)$ means that route 1 traverses link a_1. Likewise for $r_2(a_2,a_3,a_4)$ and $r_3(a_2,a_3,a_5)$.

While the above route-based specification can also characterize the HV traveler flows, it is not sufficient to characterize SAV traveler flow. This is because HVs are non-shared, thus each vehicle and the traveler in the vehicle have the same OD. With ridesharing, an SAV can take multiple travelers along its route. The ODs of an SAV and an SAV traveler can be different. An SAV traveler may be picked up (from his/her origin) in the middle of an SAV route and dropped off (at his/her destination) before the SAV route ends. This suggests the need to specify a separate network for SAV traveler flows from the vehicle route network. Inspired by the transit assignment literature (De Cea and Fernández 1993; Szeto and Jiang 2014), the separate network in this paper is built on the notion of section, which we introduce below.

Definition 1. *Section. A section $l \in L_{ij}$ is associated with an SAV traveler OD (i, j) and defined by a sequence of zones visited while the SAV traveler moves from i to j. The sequence starts from i, ends at j, and must be traversed by at least one SAV route. If multiple SAV routes exist that traverse a section, SAV travelers of the section can take any of those SAV routes.*

The requirement that a section must be traversed by at least one SAV route ensures the usability of the section. We use Fig. 1(c) to illustrate how sections are constructed given SAV traveler ODs and SAV routes shown in Fig. 1(b). Two sections, l_1 and l_2, are associated with SAV traveler OD (i_1,i_3). l_1 is defined by zone sequence $i_1 \rightarrow i_3$ and traversed by route $r_1(a_1)$. l_2 is defined by zone sequence $i_1 \rightarrow i_2 \rightarrow i_3$ and traversed by routes $r_2(a_2,a_3,a_4)$ and $r_3(a_2,a_3,a_5)$. One section, l_3, is associated with SAV traveler OD (i_1,i_2). l_3 is defined by zone sequence $i_1 \rightarrow i_2$ and traversed by routes $r_0(a_2)$, $r_2(a_2,a_3,a_4)$, and $r_3(a_2,a_3,a_5)$. One section, l_4, is associated with SAV traveler OD (i_2,i_3). l_4 is defined by zone sequence $i_2 \rightarrow i_3$ and traversed by routes $r_2(a_2,a_3,a_4)$, $r_3(a_2,a_3,a_5)$, $r_4(a_3,a_4)$, and $r_5(a_3,a_5)$.

The above illustration makes it clear that an SAV route can traverse multiple sections. For example, route $r_2(a_2,a_3,a_4)$ traverses sections l_2, l_3, and l_4 in Fig. 1. This is important as SAV travelers of different sections will compete for seats in the SAVs whose route traverses these sections. Below we introduce the notion of competing section to characterize the competition between two sections.

Definition 2. *Competing section. Section $l' \in L$ is a competing section of section $l \in L$* if *l' and l are traversed by a common SAV route, and either of the following conditions is satisfied. A binary indicator $\chi_{ll'}$ is used to show if l' is a competing section of l.*

(a) l' and l have the same origin but different destinations. SAV travelers of the two sections start from the same zone and compete for seats of SAVs whose route traverses both sections. In this case, l and l' are mutually competing: $\chi_{ll'} = \chi_{l'l} = 1$. For example, l_2 and l_3 in Fig. 1(c) are mutually competing.

(b) On a common SAV route that traverses both l and l', the origin of l is between the origin and the destination of l'. Thus, travelers of section l' using the SAV route limit the available seats for travelers of section l boarding SAVs on the same route. In this case, $\chi_{ll'} = 1$ but $\chi_{l'l} = 0$. For example, l_2 in Fig. 1(c) is a competing section of l_4 but not vice versa.

3. Problem statement

Before delving into model formulation, this section provides a conceptual description of the TNC decisions and SAV flow (Section 3.1) and the SAV/HV traveler decisions and flow (Section 3.2).

3.1. TNC decisions and SAV flow

We consider that a TNC centrally decides on the SAV allocation (to the three movement states illustrated below), routing, fleet size, and fare. The objective is to maximize profit anticipating traveler reactions which collectively result in equilibrium SAV/HV market shares and road congestion with a mixed flow of the two vehicle types. The TNC's profit is revenue minus cost. The cost comprises three components which are endogenously determined: 1) SAV fleet ownership cost; 2) SAV en-route operating cost; and 3) SAV parking cost. Quantification of these costs requires characterizing SAV flows, as described below.

The movement of an SAV can be in one of three states: in-service, pickup, and relocation, denoted as $s \in S = \{I, II, III\}$. For an SAV, an in-service state is followed by a pickup or a relocation state. A pickup or a relocation state must be followed by an in-service state. An SAV only carries travelers while in *in-service* state, but not in pickup or relocation state. An SAV starts its in-service state ($s = I$) when the TNC dispatches the SAV on a route to pick up and drop off travelers. Some travelers may be picked up at the starting zone of the in-service state; other travelers are picked up as the SAV is in the middle of the route. All travelers will be dropped off no later than the SAV reaches the end of the route, i.e., the zone where the in-service state ends.

Along the route while in in-service state, the SAV may pick up and drop off one or multiple travelers. At the end of the route, the SAV exits the in-service state and faces two choices:

(a) Remaining in the current zone, waiting to be matched with future traveler(s) from any zone (including the current zone) and then moving unoccupied to that zone to pick up the matched traveler(s). The movement is referred to as the *pickup* state ($s = II$). While waiting to be matched, we assume that the SAV will search for a parking spot in the current zone, thus incurring a parking search cost. The parking search terminates when a parking spot is found, or the SAV is matched with new traveler(s), whichever comes sooner. Once matched with a traveler, the SAV incurs a distance-based operating cost for the unoccupied trip to pick up the traveler.

(b) Relocating from the current zone to a new zone based on anticipated demand, where the next in-service state of the SAV starts. The movement is referred to as the *relocation* state ($s = III$). During relocation, the SAV does not pick up travelers. The relocating SAV incurs a distance-based operating cost for the unoccupied trip to the new zone. Note that the SAV may be matched with new traveler(s) from the zone it relocates to before arriving at the zone. If the SAV is unmatched upon arriving at the zone, the SAV will search for parking in the zone and will incur a parking search cost. The parking search terminates when a parking spot is found, or the SAV is matched with new traveler(s) in the zone, whichever comes sooner.

The TNC's allocation of SAVs to different movement states and routing in the road network is represented by decision variable y_r^s which signifies SAV flow on route r in movement state s. While it is possible to observe intra-zone SAV flows in the pickup state ($y_r^{II} \geq 0,\ O(r) = D(r)$ where $O(r)$ and $D(r)$ denote the origin and destination zones of route r), we consider that in-service and relocating SAVs do not contribute to intra-zone SAV flows ($y_r^I = y_r^{III} = 0,\ O(r) = D(r)$).

Note that SAV flows in the three movement states are interconnected in two ways. First is the SAV flow conservation at each zone $i \in Z$. That is, the total incoming in-service SAV flow destined for i should equal the total outgoing pickup/relocation SAV flows originating from i (Fig. 2(a)). In addition, the total outgoing in-service SAV flow originating from i should equal the total incoming pickup/relocation SAV flows destined for i (Fig. 2(b)). Note that in both Fig. 2(a) and Fig. 2(b), symbol "r" is a general notation for SAV routes. Second, the SAV fleet size is determined by the total SAV flows in the three movement states during an analysis period.

Specific for in-service SAVs, as mentioned in section 2 an in-service SAV can pick up not only travelers originating from the origin of the SAV route, but also travelers originating from other zones that the SAV route goes through. In this paper, "an SAV route going through a zone" means that the zone is an *intermediate* zone of the route. A "going-through" SAV can pick up a traveler only if the SAV is matched with the traveler no later than the time the SAV arrives at the origin zone of the traveler, assuming that an in-service SAV will not incur stopping at an intermediate zone other than picking up the traveler. An indicator variable g_{ri} is introduced below to describe the possibility that travelers originating in zone i can be picked up by in-service SAVs on route r which goes through i.

$$g_{ri} = 0.5\ \zeta_{ri}[1 + sgn(t_{ri} - \omega_i^y)], \forall r \in R; i \in Z \tag{1}$$

where ζ_{ri} is a route-zone correspondence indicator equal to 1 if zone i is an intermediate zone on route r. t_{ri} is the SAV travel time from the origin of route r to zone i. As an SAV which can pick up travelers in zone i may be already in the middle of route r, t_{ri} represents a conservative estimate of the SAV travel time (which probably is the best we can do in a static setting). ω_i^y is the waiting time of an SAV in matching with travelers who originate at zone i. More precisely, the waiting time of such an SAV is the amount of time it takes for the TNC to receive ride requests from a traveler group originating from zone i and match the traveler group with the SAV. The notion of a traveler group, which is given next in section 3.2, is reflective of the one (SAV)-to-many (riders) nature of autonomous ridesharing. How ω_i^y is calculated will be further discussed in detail in section 4.1.1.

Provided that $\zeta_{ri} = 1$, g_{ri} can take three possible values:

1) if $t_{ri} > \omega_i^y$, $g_{ri} = 1$, i.e., SAVs on route r are matched with travelers originating from zone i before the SAVs arrives at i. Thus the SAVs can pick up traveler(s) originating from zone i;
2) if $t_{ri} < \omega_i^y$, $g_{ri} = 0$, i.e., SAVs on route r are matched with travelers originating from zone i later than the SAVs arrives at i. Thus the SAVs cannot pick up traveler(s) originating from zone i;
3) if $t_{ri} = \omega_i^y$, $g_{ri} = 0.5$, i.e., SAVs on route r are matched with travelers originating from zone i exactly when the SAVs arrives at i. In this case, a 50% possibility is considered.

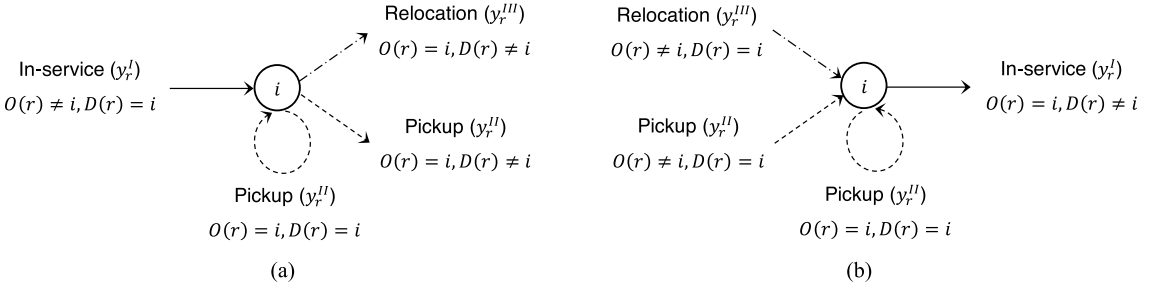

Fig. 2. SAV flow conservation in a zone with respect to: (a) incoming in-service SAVs, and (b) outgoing in-service SAVs.

3.2. SAV/HV traveler decisions and flow

We consider that each traveler can choose either SAV or HV to make a trip. Assuming an exogenous total travel demand Q_{ij} for each OD (i, j) per unit time, the endogenous demand for each vehicle type (Q_{ij}^m, $m \in M$) is based on the generalized travel costs perceived using SAV/HV, which are itemized below.

An SAV traveler trip consists of two stages: a waiting stage and a follow-up en-route travel stage. The waiting stage starts from an SAV traveler sending a ride request to the TNC through an online platform. The SAV traveler waits to be first matched with an SAV and subsequently to meet the matched SAV. Thus, two waiting times need to be specified. The first waiting time for an SAV traveler at his/her origin zone, i.e., the waiting time in matching, depends on the number of travelers to be matched in the zone and the rate of the travelers being matched.

Specification of the matching rate needs to account for ridesharing, which allows multiple travelers originating from a zone to be matched with an SAV that either originates from or traverses the zone if the SAV has available seats. To capture this, *one (SAV)-to-many (riders) matching* is proposed by introducing the notion of a *traveler group*, which refers to a group of travelers originating from the same zone and may have the same or different destinations. The matching rate for SAV travelers in a zone is measured as the number of traveler groups matched per unit time in the zone. Under the traveler group notion, while being matched each traveler in a group should wait until everyone in the group is matched with the same SAV. The notion also means that the matching of an SAV is with a traveler group. The SAV should wait until it is matched with all travelers in a traveler group. Thus, at equilibrium the matching rate in a zone, which is the number of traveler groups matched per unit time, should equal the number of SAVs matched per unit time in the zone.

After being matched, the second waiting time for an SAV traveler occurs while (s)he waits for the matched SAV to come. As a matched SAV may start its service from the same zone as the origin of the SAV traveler or just go through the SAV traveler's origin zone, which will incur different waiting time, both possibilities need to be considered in the calculation of the second waiting time. In addition, extra waiting time may arise for the SAV traveler due to limited seat capacity of the matched SAV. Once picked up by an SAV, the SAV traveler enters the en-route travel stage. Travel cost at this stage consists of in-vehicle travel time cost and fare, both depending on the SAV route. In-vehicle travel time is further affected by traffic congestion.

While SAV routing is considered as the TNC decision, the distribution of SAV travelers of an OD among different sections served by SAV routes can be under two plausible philosophies. One philosophy is that the distribution is under full control of the TNC. The TNC dispatches SAVs to different routes to accommodate travelers, and also allocates travelers to different sections served by the SAV routes. Under this philosophy, SAV travelers will not have a choice on what section to take. The TNC will make the section choice for the traveler. An alternative philosophy is that the TNC provides SAV travelers (e.g., through a mobile application) with section options to choose from. This corresponds to a plausible, informed future especially given the multiple items involved in generalized travel cost of taking SAV: waiting time in matching, waiting time to meet the matched vehicle, potential extra waiting time due to SAV seat capacity limits, in-vehicle travel time, and fare. With section choices, SAV travelers are offered more flexibilities. The provision of routing flexibilities can be important as the TNC competes with HVs for travelers. Thus, it probably would be more favorable than not giving SAV travelers section options. In view of this, we opt for the second philosophy in the paper, which leads to the notion of ARUE as defined below. We note that the consideration of ARUE is also in line with how routing choice of riders is modeled in the existing studies on human-driven ridesharing as reviewed in Table 1.

Definition 3. *Autonomous Ridesharing User Equilibrium (ARUE). For each OD, it is assumed that each SAV traveler can make choice among a set of sections, about which information would be provided by the TNC. As a consequence, an ARUE is considered that in the long term no SAV traveler on an OD can reduce its generalized travel cost by unilaterally switching to a different section other than his/her choice.*

For an HV traveler, characterizing his/her trip is simpler than the trip of an SAV traveler. A trip of an HV traveler consists of two stages: an en-route stage and a subsequent parking stage when the traveler arrives at the destination zone. At the en-route stage, an HV traveler drives from the origin zone to the destination zone using a route. The en-route cost of the traveler is the sum of vehicle operating cost and in-vehicle travel time cost. Vehicle operating cost is distance based. In-vehicle travel time depends on traffic congestion on the route, which is affected by not only the mixed SAV/HV flow, but road capacity improvement due to shorter headways of SAVs than HVs. Assuming that HV travelers have full information on en-route cost in the long term, the HV traveler routing is modeled following the user equilibrium (UE) principle.

Upon arriving at the destination zone $i \in Z$, an HV traveler will cruise within i searching for parking. The parking cost of an HV traveler at i comprises two components: 1) distance-based HV operating cost during parking search, and 2) in-vehicle travel time cost during parking search. The two components are endogenous depending on total parking demand from HVs/SAVs and parking capacity at i which is shared by HVs/SAVs.

4. Formulation of the multimodal autonomous ridesharing user equilibrium (MARUE)

With the conceptual description of the network representation and TNC/traveler decisions in sections 2–3, this section formulates MARUE which consists of three components: ARUE for SAV travelers (section 4.1), UE for HVs (section 4.2), and endogenous market share of each vehicle type (section 4.3). Section 4.4 formalizes the overall MARUE and provides proof of its existence.

4.1. Autonomous ridesharing user equilibrium (ARUE) for SAV travelers

As discussed in section 3.2, it is assumed that SAV travelers of each OD are assigned to different sections under ARUE, which is formalized by complementarity constraint (2) and Eq. (3):

$$0 \le q_l \perp h_l - H_{ij} \ge 0, \forall l \in L_{ij};\ (i,j) \in \Omega \tag{2}$$

$$\sum_{l \in L_{ij}} q_l = Q_{ij}^m, \forall (i,j) \in \Omega;\ m = SAV \tag{3}$$

where q_l is SAV traveler flow of section l. h_l is the generalized travel cost of SAV travelers of section l (Eq. (4)). Complementarity constraint (2) means that at equilibrium no SAV traveler takes a section that has a larger generalized travel cost than the minimum generalized travel cost of the OD (H_{ij}). Eq. (3) expresses SAV traveler flow conservation: the sum of SAV traveler flow on all sections connecting an OD equals the total SAV traveler demand for the OD.

$$h_l = \gamma_1 \varpi_{O(l)} + \gamma_1 (\eta_l + \widetilde{\eta}_l) + \gamma_2^m t_l + f_l, \forall l \in L; m = SAV \tag{4}$$

in which $\varpi_{O(l)}$ represents the average waiting time due to matching and meeting at the origin of l (see section 4.1.1). $(\eta_l + \widetilde{\eta}_l)$ is the total extra waiting time due to limited SAV seat capacity for an SAV traveler on l (see section 4.1.2). t_l is the in-vehicle travel time on l. f_l is the fare charged by the TNC on l (see section 4.1.3). γ_1 and γ_2^m (m= *SAV*) are SAV traveler VOTs for waiting and in-vehicle time.

4.1.1. Waiting time due to matching and meeting

Recalling in section 3.2 that due to the possibility of multiple travelers matched with one SAV in a zone, consideration of *one (SAV)-to-many (riders) matching* is needed. In this section, we derive in sequence: 1) the waiting time in matching of an SAV traveler and an SAV by introducing a one-to-many matching function; 2) the total waiting time of an SAV traveler in matching and meeting the matched SAV.

To derive the SAV traveler waiting time in matching, we start by expressing the number of SAV travelers originating from zone i per unit time (n_i^q) and the SAV flow that can serve those travelers ($\overline{n}_i^y$) as Eqs. (5)-(6):

$$n_i^q = \sum_{l \in L: O(l) = i} q_l, \forall i \in Z \tag{5}$$

$$\overline{n}_i^y = \sum_{r \in R: O(r) = i} y_r^I + \sum_{r \in R: O(r) \ne i} g_{ri} \left(y_r^I - \frac{1}{\kappa} \sum_{l \in L} \epsilon_{li} q_{lr} \right), \forall i \in Z \tag{6}$$

where κ is the number of seats in an SAV (i.e., SAV size). ϵ_{li}) is a section-zone correspondence indicator equaling 1 if zone i is an intermediate zone on section l. q_{lr} denotes SAV traveler flow of section l and using SAV route r. The calculation of q_{lr} is discussed later in section 4.1.2.

The right-hand side (RHS) of Eq. (5) is the sum of SAV travelers of all sections originating from zone i. In Eq. (6), the RHS decomposes the SAV flow that can serve travelers originating from zone i into two parts. The first part is the in-service SAV flow originating from i. The second part is the in-service SAV flow which goes through zone i, without incurring SAV waiting (as governed by g_{ri} defined in section 3.1). The subtracted term in the parentheses uses κ to convert the number of occupied seats when the going-through SAVs arrive at zone i to the equivalent occupied SAV flow.

The notion of a traveler group introduced in section 3.2 intends to capture the nature of one-to-many matching. Intuitively, the rate of matching in a zone depends on the number of traveler groups and the number of SAVs in the zone, and the extent of search each traveler group and each SAV perform during matching. Following Petrongolo and Pissarides (2001), we formalize the extent of search as *search intensity* as below.

Definition 4. *Search intensities of a traveler group and an SAV. In ridesharing matching, the search intensity of a traveler group is the group size (i.e., the number of travelers in the group), because each traveler is considered to perform individual search for an SAV without coordinating with others in the group. The search intensity of an SAV is the maximum number of traveler groups that can be potentially accommodated by the SAV, which depends on the traveler group size and the SAV seat capacity.*

The search intensity of a traveler group in zone i(σ_i^q) can be expressed by Eq. (7). Basically, σ_i^q is obtained by dividing the total number of SAV travelers originating from the zone per unit time by the SAV flow that can serve those travelers. The min and max operators constrain that the size of a traveler group should be between 1 and the number of seats in an SAV (κ).

$$\sigma_i^q = \min \left\{ \kappa, \max \left\{ 1, \frac{n_i^q}{\overline{n}_i^y} \right\} \right\}, \forall i \in Z \tag{7}$$

Knowing the search intensity (i.e., size) of a traveler group, the number of SAV traveler groups originating from zone i per unit time is n_i^q / σ_i^q. At static equilibrium, all these traveler groups should be matched with SAVs. Therefore, the number of SAVs matched in zone i per unit time, n_i^y, is:

$$n_i^y = \frac{n_i^q}{\sigma_i^q}, \forall i \in Z \tag{8}$$

According to Definition 4, the search intensity of an SAV in zone i (σ_i^y), i.e., the maximum number of traveler groups an SAV can potentially accommodate in the zone, is expressed as Eq. (9):

$$\sigma_i^y = \frac{\kappa}{\sigma_i^q}, \forall i \in Z \tag{9}$$

Following Petrongolo and Pissarides (2001), the matching rate of a zone i,$\mathscr{m}_i$, is specified as a function of the total search intensity of all traveler groups and the total search intensity of all SAVs that are waiting to be matched in the zone. The total search intensity of all traveler groups (respectively, SAVs) of the zone is the search intensity of one traveler group (respectively, SAV) multiplied by the number of traveler groups (respectively, SAVs) waiting to be matched in the zone, $\mathscr{N}_i^q$ (respectively, $\mathscr{N}_i^y$). This is:

$$\mathscr{m}_i = \mathscr{M}_i(\sigma_i^q \mathscr{N}_i^q, \sigma_i^y \mathscr{N}_i^y), \forall i \in Z \tag{10}$$

$\mathscr{N}_i^q$ can be expressed using Little's law: $\mathscr{N}_i^q = (n_i^q/\sigma_i^q)\omega_i^q$. As mentioned earlier, n_i^q/σ_i^q is the number of traveler groups matched per unit time. ω_i^q is the waiting time of an SAV traveler group in matching. Similarly applying Little's Law to SAVs leads to $\mathscr{N}_i^y = n_i^y \omega_i^y$, where n_i^y is the number of SAVs matched per unit time and ω_i^y is the waiting time of an SAV in matching. Replacing $\mathscr{N}_i^q$ and $\mathscr{N}_i^y$ in Eq. (10) by $(n_i^q/\sigma_i^q)\omega_i^q$ and $n_i^y \omega_i^y$, we obtain:

$$\mathscr{m}_i = \mathscr{M}_i(n_i^q \omega_i^q, \sigma_i^y n_i^y \omega_i^y), \forall i \in Z \tag{11}$$

With no loss of generality, we consider the Cobb-Douglas form for $\mathscr{m}_i$, which is used in existing non-shared ridehailing literature (Yang et al., 2010; Yang and Yang 2011; He and Shen 2015; Zha et al., 2016; Wang et al., 2016; Xu et al., 2017).

$$\mathscr{m}_i = B_i(n_i^q \omega_i^q)^{b_1}(\sigma_i^y n_i^y \omega_i^y)^{b_2}, \forall i \in Z \tag{12}$$

where b_1 and b_2 are matching rate elasticities. It is generally expected that b_1,$b_2 \in (0, 1]$. If $b_1 + b_2 > 1 \quad (= 1, \text{or} < 1)$, the matching function exhibits increasing (constant, or decreasing) returns-to-scale. $B_i > 0$ is a zone-specific constant reflecting the meeting location properties, e.g., point meeting as for taxi stands (larger B_i) versus zonal meeting as for ridehailing cars which cruise on streets to find riders (smaller B_i).

Following the description of equilibrium matching rate in section 3.2, we have $\mathscr{m}_i = n_i^q/\sigma_i^q = n_i^y$. By replacing $\mathscr{m}_i$ by n_i^q/σ_i^q and using Eq. (9), simple algebra on Eq. (12) yields the waiting time function of travelers as shown in Eq. (13). In Eq. (13), traveler waiting time in a zone is associated with the traveler group size σ_i^q, the SAV traveler flow originating from the zone n_i^q, and the number of SAVs to be matched in the zone $n_i^y \omega_i^y$. Similarly for the SAV waiting time (Eq. (14)).

$$\omega_i^q = (\kappa)^{-\frac{b_2}{b_1}}(\sigma_i^q)^{\frac{b_2-1}{b_1}}\left[(B_i)^{-\frac{1}{b_1}}(n_i^q)^{\frac{1-b_1}{b_1}}(n_i^y \omega_i^y)^{-\frac{b_2}{b_1}}\right], \forall i \in Z \tag{13}$$

$$\omega_i^y = (\sigma_i^y)^{-1}\left[(B_i)^{-\frac{1}{b_2}}(n_i^y)^{\frac{1-b_2}{b_2}}(n_i^q \omega_i^q)^{-\frac{b_1}{b_2}}\right], \forall i \in Z \tag{14}$$

The terms outside the brackets in Eqs. (13) and (14), i.e., $(\kappa)^{-\frac{b_2}{b_1}}(\sigma_i^q)^{\frac{b_2-1}{b_1}}$ and $(\sigma_i^y)^{-1}$, are less than or equal to one given that $\sigma_i^q, \sigma_i^y \in [1, \kappa]$ and $b_1, \quad b_2 \in (0, 1]$. This suggests that holding the bracket terms constant, the waiting times of a traveler group and an SAV in matching will be reduced (at least not increase) with ridesharing.

Eqs. (13)-(14) together with Eqs. (7)-(9) suggest that ω_i^q and ω_i^y depend on n_i^q and $\overline{n}_i^y$. SAV traveler flows captured by n_i^q are accommodated by in-service SAV flows (see section 4.1.2). Eq. (6) suggests that $\overline{n}_i^y$ is also determined by in-service SAV flows. As discussed in section 3.1 and will be made further clear in section 5, in-service SAV flows are constrained by the SAV fleet size and depend on how the TNC allocates SAVs to in-service, pickup, and relocation states. Thus, the waiting times of an SAV traveler group and an SAV in matching are impacted by the TNC's decision-making.

It is worth noting that all SAVs involved in matching at a zone i, as shown in Eq. (6), are in-service state. Thus, when matching is done, an SAV – no matter matched or not – will move "in-service": for matched SAVs, they will pick up their matched SAV travelers and move; for unmatched SAVs, they will also move like the matched SAVs, though not picking up SAV travelers from zone i. Also, Eq. (6) suggests that unmatched SAVs could be of two types: 1) those originating from zone i, in which case an unmatched SAV will depart from zone i without having travelers onboard; and 2) those moving through zone i, in which case an unmatched SAV may have some travelers who originate from other zones onboard while moving through zone i. While considering the continuous movement for the latter type of unmatched SAVs is natural as those SAVs are already en route, one might think that the former type of unmatched SAVs could stay in the zone. However, this would be inconsistent with Eq. (6) that all SAVs involved in matching (regardless of the matching outcome) are in the "in-service" movement state. On the other hand, if there are some unmatched SAVs moving "in-service" but empty, they will incur cost but do not generate revenue. As our overall problem is profit maximization (see section 5), the optimization process will try to minimize such unmatched SAVs, although some of the empty "in-service" movements could be beneficial at the system level for meeting traveler demand at downstream zones of the SAV routes. Some numerical investigations of empty in-service SAV

movements will be performed in section 7.1.

The following two propositions further explore the relationship between traveler group and SAV waiting times in matching, and parameters b_1 and b_2 in the Cobb-Douglas matching function.

Proposition 1. *Given the SAV traveler flow originating from zone i (n_i^q) and SAV waiting time in matching (ω_i^y), the waiting time of an SAV traveler group in matching (ω_i^q) is non-decreasing with ridesharing vs. without ridesharing if $b_2 > 0.5$. In addition, ω_i^q becomes larger with larger σ_i^q,* i.e., *more intense ridesharing. Similarly for ω_i^y given n_i^q and ω_i^q.*

Proof. See Appendix 1. □

Proposition 2. *Given the traveler group search intensity (σ_i^q) and SAV waiting time in matching (ω_i^y) in a zone i, the waiting time of an SAV traveler group in matching (ω_i^q) increases with the SAV traveler flow originating from zone i (n_i^q) if the Cobb-Douglas matching function exhibits decreasing returns-to-scale and $n_i^q > 1$. Similarly for ω_i^y given σ_i^q and ω_i^q.*

Proof. See Appendix 1. □

Once the matching ends, travelers originating from zone i may need to wait further for meeting the matched SAVs. As shown in Eq. (6), such SAVs either originate from or go through i. We derive ϖ_i, the average waiting time of an SAV traveler originating from zone i due to matching and meeting. ϖ_i is calculated as the sum of total traveler waiting time for SAVs both originating from and going through zone i (termed TTW_i^+ and TTW_i^-) divided by the SAV traveler flow originating from the zone:

$$\varpi_i = \frac{TTW_i^+ + TTW_i^-}{\sum_{l \in L:O(l)=i} q_l}, \forall i \in Z \tag{15}$$

We need to further express TTW_i^+ and TTW_i^-. For TTW_i^+, it is the SAV traveler flow originating from zone i and taking SAVs that also originate from i (i.e., $\sum_{r \in R:O(r)=i} \sum_{l \in L:O(l)=i} q_{lr}$), multiplied by the average waiting time incurred by each of these travelers. Since SAVs originating from i consist of those moving to i in pickup state ($s = II$) and in relocation state ($s = III$), the average waiting time of a traveler is the weighted average of waiting time for taking SAVs moving to i in the two states, weighted by the SAV flows in the two states. The waiting time for SAVs in pickup state is the sum of matching time and pickup time, i.e., $\omega_i^q + t_r$. The waiting time for SAVs in relocation state is the maximum of matching time and relocation time, i.e., $max\{\omega_i^q, t_r\}$. Eq. (16) gives the final expression for TTW_i^+. A small positive number ε is added to avoid zero in the denominator.

$$TTW_i^+ = \frac{\sum_{r \in R:D(r)=i} \left[y_r^{II} (\omega_i^q + t_r) + y_r^{III} max\{\omega_i^q, t_r\} \right]}{\sum_{r \in R:D(r)=i} \left(y_r^{II} + y_r^{III} \right) + \varepsilon} \sum_{r \in R:O(r)=i} \sum_{l \in L:O(l)=i} q_{lr}, \forall i \in Z \tag{16}$$

TTW_i^- is computed in Eq. (17) as the SAV traveler flow originating from zone i and taking SAVs that go through i, multiplied by the average waiting time incurred by each of these travelers. We use ζ_{ri} because zone i must be an intermediate zone on the SAV route. $max\{\omega_i^q, t_{ri}\}$ reflects the fact that an SAV traveler can only be picked up when the traveler is matched and the SAV has arrived at zone i from its origin.

$$TTW_i^- = \sum_{r \in R} \zeta_{ri} max\{\omega_i^q, t_{ri}\} \sum_{l \in L:O(l)=i} q_{lr}, \forall i \in Z \tag{17}$$

Eqs. (18)-(19) show how t_r and t_{ri} are calculated, where δ_{ar} is the link-route correspondence indicator equaling 1 if link a lies on route r. δ_{ar}^i is a link-route-zone correspondence indicator equating 1 if: 1) link a lies on route r; 2) zone i lies on route r; 3) the end of link a is no later than i on route r.

$$t_r = \sum_{a \in A} \delta_{ar} t_a, \forall r \in R \tag{18}$$

$$t_{ri} = \sum_{a \in A} \delta_{ar}^i t_a, \forall r \in R; i \in Z \tag{19}$$

4.1.2. Waiting time due to limited SAV seat capacity

As mentioned in section 3.2, in addition to waiting for matching and meeting, another type of waiting may occur when there are not enough seats provided by SAVs. To capture this, we establish the following SAV seat capacity constraint on each section l (measured at the origin of section l).

$$q_l + \widetilde{q}_l \leq \kappa \left(\sum_{r \in R:O(r) \neq O(l)} \lambda_{lr} g_{r,O(l)} y_r^I + \sum_{r \in R:O(r)=O(l)} \lambda_{lr} y_r^I \right), \forall l \in L \tag{20}$$

where $\widetilde{q}_l$ is the portion of SAV traveler flow of competing sections of section l and using common routes that traverse l, and will be specified below. λ_{lr} is a section-route correspondence indicator equaling 1 if route r traverses section l, and 0 otherwise.

The RHS of Eq. (20) denotes total SAV seat flow on section l, which equals the number of seats per SAV (κ) times the total SAV flow

on the section. Inside the parentheses, the first term refers to the in-service SAV flow going through section l. $g_{r,O(l)}$, as defined in section 3.1, is used to ensure that only those going-through SAVs that can pick up travelers at the origin of section l are counted. The second term represents the in-service SAV flow whose routes start at the origin of section l.

The left-hand side (LHS) of Eq. (20) denotes total traveler flow competing for SAV seats on section l, which is SAV traveler flow of section l (q_l), plus SAV traveler flow of competing sections of section l and using common routes that traverse l ($\widetilde{q}_l$). $\widetilde{q}_l$ is calculated as:

$$\widetilde{q}_l = \sum_{l' \in L \setminus l} \chi_{ll'} \sum_{r \in R} \lambda_{lr} q_{l'r}, \forall l \in L \tag{21}$$

where $q_{l'r}$ is the SAV traveler flow of section l' and using SAV route r, which is computed in Eq. (22). The basic idea of Eq. (22) is to assign SAV travelers of a section to different routes based on SAV flows of these routes. In Eq. (22), π_{lr} is the SAV flow of route r that traverses section l. π_{lr} is calculated by Eq. (23), with the two terms already explained in Eq. (20). A small positive number ε in the denominator is added to avoid zero when $\pi_l = 0$. In Eq. (24), π_l is the total SAV flows on all routes traversing section l. It can be easily seen that π_l is equal to the parenthesized term on the RHS of Eq. (20).

$$q_{lr} = \frac{\pi_{lr}}{\pi_l + \varepsilon} q_l, \forall l \in L; r \in R \tag{22}$$

$$\pi_{lr} = \begin{cases} \lambda_{lr} g_{r,O(l)} y_r^l & \text{if } O(r) \neq O(l) \\ \lambda_{lr} y_r^l & \text{if } O(r) = O(l) \end{cases}, \forall l \in L; r \in R \tag{23}$$

$$\pi_l = \sum_{r \in R} \pi_{lr}, \forall l \in L \tag{24}$$

Following Larsson and Patriksson (1999), constraint (20) represents a side constraint of ARUE. Therefore, its Lagrange multiplier, η_l, is used in the complementarity constraint (25). η_l can be interpreted as the extra waiting time for SAV travelers of section l due to limited SAV seat capacity on the section. Obviously, $\eta_l = 0$ when $\kappa\pi_l - q_l - \widetilde{q}_l > 0$.

$$0 \leq \eta_l \perp \kappa\pi_l - q_l - \widetilde{q}_l \geq 0, \forall l \in L \tag{25}$$

An SAV route may traverse multiple sections. Therefore, the waiting time for SAV travelers of section l due to limited SAV seat capacity arises not only from η_l, but from similar waiting time for SAV travelers of competing sections ($\widetilde{\eta}_l$). The calculation of $\widetilde{\eta}_l$ is shown in Eq. (26). For a competing section l', its contribution to the extra waiting time for SAV travelers of section l is $\eta_{l'}$ times the proportion of SAV flow on common routes that traverse both sections l and l', i.e., $\sum_{r \in R} \lambda_{lr}\lambda_{l'r}\pi_{lr}$, in the total SAV flows on all routes traversing l, i.e., π_l.

In Eq. (26), a small number ε is added to both the denominator and the numerator. The addition of ε to the denominator is to avoid zero in the denominator when no SAV traverses section l ($\pi_l = 0$). The addition of ε to the numerator is to prevent $\widetilde{\eta}_l = 0$, which would occur (without the ε in the numerator) when $\pi_l = 0$ (and subsequently $\pi_{lr} = 0$, $\forall r$), but can be problematic. This is because $\pi_l = 0$ means that $q_l = 0$ (and $\widetilde{q}_l = 0$) from Eq. (25). In other words, there is no SAV traveler flow of section l. However, $\widetilde{\eta}_l = 0$ contributes to a small generalized cost of using section l, which contradicts the fact that section l has no SAV traveler. Adding ε to the numerator will lead to $\widetilde{\eta}_l = \sum_{l' \in L \setminus l} \chi_{ll'} \eta_{l'}$, which is the largest possible value of $\widetilde{\eta}_l$ as the proportion term ($\sum_{r \in R} \lambda_{lr}\lambda_{l'r}\frac{\pi_{lr}+\varepsilon}{\pi_l+\varepsilon}$) takes value 1.

$$\widetilde{\eta}_l = \sum_{l' \in L \setminus l} \chi_{ll'} \eta_{l'} \sum_{r \in R} \lambda_{lr}\lambda_{l'r} \frac{\pi_{lr} + \varepsilon}{\pi_l + \varepsilon}, \forall l \in L \tag{26}$$

4.1.3. In-vehicle time and fare

Besides waiting time, in-vehicle time and fare need to be quantified. Eqs. (27)-(28) compute the average in-vehicle travel time (t_l) and the average fare (f_l) incurred by SAV travelers of section l. Same as the treatment in Eq. (26), t_l and f_l come from weighted averages over all routes traversing the section, weighted by SAV flows on those routes. The addition of a small number ε to the denominator and to the numerator is similarly justified as that in Eq. (26).

$$t_l = \sum_{r \in R} \frac{\pi_{lr} + \varepsilon}{\pi_l + \varepsilon} \lambda_{lr} t_{lr}, \forall l \in L \tag{27}$$

$$f_l = \sum_{r \in R} \frac{\pi_{lr} + \varepsilon}{\pi_l + \varepsilon} \lambda_{lr} f_{lr}, \forall l \in L \tag{28}$$

where t_{lr} and f_{lr} represent the in-vehicle travel time and fare on a portion of route r that is section l:

$$t_{lr} = \lambda_{lr} \sum_{a \in A} \left(\delta_{ar}^{D(l)} - \delta_{ar}^{O(l)}\right) t_a, \forall r \in R, l \in L \tag{29}$$

$$f_{lr} = \lambda_{lr}\left(f_0 + f_d \sum_{a\in A}\left(\delta_{ar}^{D(l)} - \delta_{ar}^{O(l)}\right)d_a\right), \forall l \in L, r \in R \tag{30}$$

where f_0 and f_d are the constant ($/ride) and the distance-based ($/mile) fares determined by the TNC.

4.2. User equilibrium (UE) for HVs

As discussed in section 3.2, we model the routing behavior of HVs based on the UE principle (Wardrop 1952). To prevent route enumeration, we employ the link-node formulation (e.g., Ban et al., 2008).

$$0 \le x_{ai} \perp c_a + C_{D(a),i} - C_{O(a),i} \ge 0, \forall a \in A; i \in Z \tag{31}$$

$$\sum_{a\in A:O(a)=n} x_{ai} - \sum_{a\in A:D(a)=n} x_{ai} = \mathbb{Q}_{ni}^m, \forall n \in N; i \in Z; m = HV \tag{32}$$

where

$$\mathbb{Q}_{ni}^m = \left\{\begin{array}{l} 0 \; if \; n \in N \setminus Z \\ Q_{ni}^m \; if \; n \in Z \setminus \{i\} \\ -\sum_{(j,i)\in\Omega} Q_{ji}^m \; if n = i \end{array}\right\}, \forall n \in N; i \in Z; m = HV \tag{33}$$

x_{ai} is the HV flow on link a and destined to zone i, which is proportional to the corresponding HV traveler flow by an HV occupancy ratio that is assumed equal to one in this paper. c_a is the generalized travel cost using HV on link a. $C_{D(a),i}$ is the minimum generalized travel cost using HV from the end of link a to zone i at equilibrium. We conventionally set $C_{D(a),i} = 0$ if $D(a) = i$. Similarly for $C_{O(a),i}$. Q_{ni}^m is the travel demand of vehicle type m (here, HVs) from zone n (if $n \in Z$) to zone i.

The complementarity constraint (31) establishes the UE conditions for HVs. In plain words, if link a carries HV flow from any zone to zone i ($x_{ai} > 0$), then travel cost on the link plus the minimum generalized travel cost from the end of the link $D(a)$ to zone i should equal the minimum generalized travel cost from the beginning of the link $O(a)$ to zone i. Flow conservation condition of Eq. (32) ensures that the i-bound flow leaving node n minus the i-bound flow entering node n should equal the i-bound demand generated from node n, unless $n = i$.

Eq. (34) computes the generalized travel cost with HV on a link as the sum of distance-based vehicle operating cost (first term) and in-vehicle time cost (second term).

$$c_a = \left(\theta_1^m + \theta_2^m\right)d_a + \gamma_2^m t_a, \forall a \in A; m = HV \tag{34}$$

where θ_1^m and θ_2^m are respectively the fixed cost (due to depreciation of vehicle price) and the variable cost (due to insurance, fuel, and maintenance) components of the HV operating cost per unit distance. γ_2^m is traveler in-vehicle VOT using vehicle type m. d_a and t_a are length of link a and travel time on link a.

Following Noruzoliaee et al. (2018), t_a is derived using a modified BPR function (35) which endogenously models link capacity as a function of vehicle-type specific total link flows (v_a^m) and headways at maximum flow (i.e., capacity) (τ_m).

$$t_a = t_{0,a}\left[1 + \alpha_a\left(\frac{\sum_{m\in M}\tau_m v_a^m}{\tau_{HV}K_a^{HV}}\right)^{\beta_a}\right], \forall a \in A \tag{35}$$

where parameters $t_{0,a}$ and K_a^{HV} represent free-flow travel time and base capacity with only HVs on link a. α_a and β_a are the link's BPR function parameters. v_a^m for HVs and SAVs are derived in (36)-(37). Thus the congestion effect of both HVs and SAVs are accounted for in the model.

$$v_a^m = \sum_{i\in Z} x_{ai}, \forall a \in A; m = HV \tag{36}$$

$$v_a^m = \sum_{s\in S}\sum_{r\in R}\delta_{ar}y_r^s, \forall a \in A; m = SAV \tag{37}$$

The RHS of Eq. (36) aggregates HV flows destined to all zones using link a. SAV flows using link a in any movement state $s \in S$ is captured in RHS of Eq. (37).

4.3. Endogenous market shares of SAV and HV

We consider an exogenous total travel demand Q_{ij} for each OD (i, j) per unit time. The vehicle type choice of a traveler on OD (i, j) is

based on the generalized travel cost perceived using each vehicle type. Assuming that the cost perceptions are subject to error, the market share of each vehicle type Q_{ij}^m $(m \in M)$ is specified by a logit model:

$$\frac{Q_{ij}^m}{Q_{ij}} = \frac{exp\left(-\varphi U_{ij}^m\right)}{\sum_{m' \in M} exp\left(-\varphi U_{ij}^{m'}\right)}, \forall (i,j) \in \Omega; m \in M \tag{38}$$

where

$$U_{ij}^m = C_{ij} + \gamma_1 PT_j + PC_j^m, \forall (i,j) \in \Omega; m = HV \tag{39}$$

$$U_{ij}^m = H_{ij}, \forall (i,j) \in \Omega; m = SAV \tag{40}$$

In the above equations, $\varphi > 0$ is the logit scale factor (Train 2003). U_{ij}^m is the perceived generalized travel cost using vehicle type m for OD (i, j). HV users incur the equilibrium in-vehicle time and vehicle operating cost (C_{ij}), parking search time cost ($\gamma_1 PT_j$), and parking search cost (PC_j^m). We assume that HV users during parking search have the same VOT as SAV travelers when waiting for SAVs. Thus γ_1 is placed before PT_j. SAV travelers incur the equilibrium ridesharing cost (H_{ij}).

The HV operating cost during parking search in a zone i is considered a linear function of the parking search time PT_i and a (constant) vehicle speed ($\mathcal{S}_i$) during search. This is shown in Eq. (41).

$$PC_i^m = (\theta_1^m + \theta_2^m)\mathcal{S}_i PT_i \qquad \forall i \in Z;\ m = HV \tag{41}$$

Following Lam et al. (2006) and Jiang et al. (2014), we derive the parking search time in a zone as a BPR-like function of total parking demand and parking infrastructure capacity in the zone.

$$PT_i = PT_{0,i}\left[1 + \alpha_i\left(\frac{\sum_{m \in M} PD_i^m}{PK_i}\right)^{\beta_i}\right], \forall i \in Z \tag{42}$$

where $PT_{0,i}$ is the free-flow parking search time, α_i and β_i are parameters, PD_i^m is the parking demand of vehicle type $m \in M$, and PK_i is the parking infrastructure capacity, all for zone i.

Eqs. (43)-(44) show how vehicle type-specific parking demand in a zone is computed. For HVs, parking demand in zone i equals the total HV flow destined to i. The parking demand of vacant SAVs in zone i is more complicated as it depends on movement states. For vacant SAVs in zone i waiting to be matched with travelers in any zone j, and then moving to zone j in pickup state ($s = II$), demand for parking in zone i occurs only when the matching time is longer than the time to find a parking spot in zone i, i.e., $\omega_j^y > PT_i$. This is characterized by $max\{0, \omega_j^y - PT_i\}$ in Eq. (44). For vacant SAVs moving to i from another zone j in relocation state ($s = III$), demand for parking in zone i occurs only when it takes longer for the SAVs to be matched with travelers in zone i than to travel from j to i plus the parking search time in zone i, i.e., $\omega_i^y > t_r + PT_i$. This is reflected by $max\{0,\ \omega_i^y - t_r - PT_i\}$ in Eq. (44). Note further that parking demand is defined on an hourly basis, to be consistent with the hourly parking capacity PK_i in Eq. (42). Thus, if an SAV parks for more than an hour, only the first hour contributes to the hourly parking demand. This is realized by using the min functions in Eq. (44).

$$PD_i^m = \sum_{(j,i) \in \Omega} Q_{ji}^m, \forall i \in Z; m = HV \tag{43}$$

$$PD_i^m = \sum_{j \in Z}\left(\sum_{r \in R_{ij}} y_r^{II} min\left\{1,\ max\left\{0,\ \omega_j^y - PT_i\right\}\right\} + \sum_{r \in R_{ji}} y_r^{III} min\left\{1,\ max\left\{0,\ \omega_i^y - t_r - PT_i\right\}\right\}\right), \forall i \in Z; m = SAV \tag{44}$$

4.4. Overall formulation of MARUE and its existence

This section presents the overall formulation of MARUE and proves its existence. We note that sgn, max, and min functions, which are not continuously differentiable, are used in ARUE and market share specifications. For computational tractability, we first approximate these functions using Eqs. (45)-(47), where ε is a small positive number.

$$sgn(a) = a \Big/ |a| \cong a \Big/ \sqrt{a^2 + \varepsilon} \tag{45}$$

$$max\{a,b\} = 0.5(a + b + |b - a|) \cong 0.5\left(a + b + \sqrt{(b-a)^2 + \varepsilon}\right) \tag{46}$$

$$min\{a,b\} = 0.5(a + b - |a - b|) \cong 0.5\left(a + b - \sqrt{(a-b)^2 + \varepsilon}\right) \tag{47}$$

Lemma 1 below presents the nonlinear complementarity problem (NCP) formulation of MARUE. Complementarity constraints (48)-

(49) replace the flow conservation constraints of ARUE (Eq. (3)) and UE (Eq. (32)). The equivalence can be verified similar to that for traditional UE (e.g., in Facchinei and Pang (2003)). Complementarity constraint (50) satisfies the market share function (38) due to the strict positivity of $Q_{ij} exp(-\varphi U_{ij}^m)/\sum_{m' \in M} exp(-\varphi U_{ij}^{m'})$, which forces Q_{ij}^m to be strictly positive.

Lemma 1. . *NCP (P1) yields MARUE.*

(P1): NCP-MARUE

$$0 \le H_{ij} \perp \sum_{l \in L_{ij}} q_l - Q_{ij}^m \ge 0, \forall (i,j) \in \Omega; m = SAV \tag{48}$$

$$0 \le C_{ni} \perp \sum_{a \in A: O(a)=n} x_{ai} - \sum_{a \in A: D(a)=n} x_{ai} - \mathbb{Q}_{ni}^m \ge 0, \forall n \in N; i \in Z; m = HV \tag{49}$$

$$0 \le Q_{ij}^m \perp Q_{ij}^m - Q_{ij} \frac{\exp\left(-\varphi U_{ij}^m\right)}{\sum_{m' \in M} \exp\left(-\varphi U_{ij}^{m'}\right)} \ge 0, \forall (i,j) \in \Omega; m \in M \tag{50}$$

Complementarity constraints (2), (25), and (31) and definitional constraints (1), (4)-(9), (13)-(19), (21)-(24), (26)-(30), (33)-(37), (39)-(47).

Proposition 3 establishes an equivalent variational inequality (VI) problem to MARUE, which is used later in Section 6 for solving the TNC's problem since our numerical experiments find that it is more efficient to solve the VI than the NCP (P1).

Proposition 3. *VI (P2) is equivalent to NCP (P1).*

(P2): VI-MARUE

$$\begin{aligned} &\sum_{l \in L} [h_l(q_l - \widehat{q}_l) + (\kappa \pi_l - q_l - \widetilde{q}_l)(\eta_l - \widehat{\eta}_l)] + \sum_{i \in Z} \sum_{a \in A} c_a^m (x_{ai} - \widehat{x}_{ai}) \\ &+ \sum_{(i,j) \in \Omega} \left[\sum_{m=HV} \left(\gamma_1 PT_j + PC_j^m + \frac{1}{\varphi} \ln \widehat{Q}_{ij}^m \right) \left(Q_{ij}^m - \widehat{Q}_{ij}^m \right) + \frac{1}{\varphi} \sum_{m=SAV} \ln \widehat{Q}_{ij}^m \left(Q_{ij}^m - \widehat{Q}_{ij}^m \right) \right] \ge 0, \forall (\boldsymbol{q}, \boldsymbol{\eta}, \boldsymbol{x}, \boldsymbol{Q}) \in \Phi \end{aligned} \tag{51}$$

where $(\boldsymbol{q}, \boldsymbol{\eta}, \boldsymbol{x}, \boldsymbol{Q})$ *is the vector form of the corresponding variables. The variables with a hat denote the solution of the VI.* Φ *is the feasible region of the VI determined by the following constraints.*

$$q_l \ge 0, \forall l \in L \tag{52}$$

$$\eta_l \ge 0, \forall l \in L \tag{53}$$

$$x_{ai} \ge 0, \forall a \in A; \ i \in Z \tag{54}$$

$$\sum_{m \in M} Q_{ij}^m = Q_{ij}, \forall (i,j) \in \Omega \tag{55}$$

Flow conservation constraints (3) and (32) and definitional constraints of problem (P1).

Proof. See Appendix 1. □

Proposition 4 proves the existence of an equilibrium solution to MARUE under a specific condition.

Proposition 4. *Assume that a set of Lagrange multipliers* $\boldsymbol{\eta}$ *for the SAV seat capacity constraint (20) exists. Then there is at least one solution to NCP-MARUE (P1) and VI-MARUE (P2).*

Proof. See Appendix 1. □

5. Formulation of the TNC's decisions

Recall from Section 3.1 that the profit-maximizing TNC centrally decides on the SAV fleet size (F), fixed and distance-based fare rates ($\boldsymbol{f} = (f_0, \quad f_d)$), and vehicle allocation and routing ($\boldsymbol{y} = (\ldots, y_r^s, \ldots), r \in R, s \in S$). The TNC's profit is written in Eq. (56) as the total revenue (first term) minus parking cost (second term), en-route operating cost (third term), and fleet ownership cost (fourth term).

$$Profit = \sum_{l \in L} q_l f_l - \sum_{m=SAV} \sum_{i \in Z} PC_i^m - \theta_2^m \sum_{s \in S} \sum_{r \in R} d_r y_r^s - \mu F \tag{56}$$

where $\theta_2^m (m = SAV)$ is the variable cost (due to insurance, fuel, and maintenance) component of SAV operating cost per unit distance, μ is the capital cost of an SAV per unit time, and d_r is the length of route $r \in R$.

The parking cost in a zone i comes from parking search cost (PC_i^m). As shown in Eq. (57), PC_i^m depends on the state of vacant SAVs.

For vacant SAVs in pickup state waiting in zone i, parking search lasts until finding a parking spot or being matched with new traveler (s) from any zone j, whichever occurs first (as captured by $min\{PT_i,\ \omega_j^y\}$). For vacant SAVs relocating to zone i from another zone j, parking search starts only when an SAV is not matched with new traveler(s) when arriving in zone i (as captured by $max\{0,\ \omega_i^y - t_r\}$, $r \in R_{ji}$), and lasts until either a parking spot is found or the SAV picks up the matched traveler(s) (as captured by $min\{PT_i,\ max\{0,\ \omega_i^y - t_r\}\}$), whichever comes earlier.

$$PC_i^m = \theta_2^m \delta_i \sum_{j\in Z}\left(\sum_{r\in R_{ij}} y_r^{II}\min\{PT_i, \omega_j^y\} + \sum_{r\in R_{ji}} y_r^{III}\min\left\{PT_i, \max\{0, \omega_i^y - t_r\}\right\}\right)\ ,\ \forall i \in Z;\ m = SAV \tag{57}$$

Constraints (58)-(60) ensure the non-negativity of the supply attributes.

$$f_0 \geq 0 \tag{58}$$

$$f_d \geq 0 \tag{59}$$

$$y_r^s \geq 0, \forall s \in S; r \in R \tag{60}$$

The TNC's vehicle allocation and routing decisions should further satisfy SAV flow conservation constraints and service time constraints, as detailed in sections 5.1 and 5.2.

5.1. SAV flow conservation

As shown in Fig. 2(a), the total in-service SAV flow destined to a zone i should be equal to the total vacant SAV flow originating from i Eq. (61)). In addition, Fig. 2(b) suggests that the total vacant SAV flow destined to zone i must be balanced with the total in-service SAV flow originating from i (Eq. (62)). Note that Eqs. (61)-((62) are not included in the NCP (P1) or VI (P2).

$$\sum_{r\in R:D(r)=i} y_r^I = \sum_{r\in R:O(r)=i}\left(y_r^{II} + y_r^{III}\right), \forall i \in Z \tag{61}$$

$$\sum_{r\in R:D(r)=i}\left(y_r^{II} + y_r^{III}\right) = \sum_{r\in R:O(r)=i} y_r^I, \forall i \in Z \tag{62}$$

5.2. SAV time conservation

As discussed in section 3.1, SAV flows in three movement states are interconnected and connected to the SAV fleet size. Assuming a one-hour analysis period, constraint (63) establishes the relationship between SAV flow and SAV fleet size F. In an hour, F equals the total en-route SAV hours (first term) plus the total waiting SAV hours (second and third terms). En-route SAV hours include occupied, pickup, and relocation SAV hours. Waiting SAV hours are associated with vacant SAVs. Specifically, for vacant SAVs in zone i waiting to be matched with travelers from any zone j and then picking up the matched travelers, the SAV waiting time is ω_j^y. For vacant SAVs relocating from zone j to another zone i, the SAV waiting time in zone i is non-zero only when matching with travelers ends after arriving in i (as captured by $max\{0,\ \omega_i^y - t_r\}, r \in R_{ji}$).

$$F = \sum_{s\in S}\sum_{r\in R} y_r^s t_r + \sum_{j\in Z}\sum_{i\in Z}\left(\sum_{r\in R_{ij}} y_r^{II}\omega_j^y + \sum_{r\in R_{ji}} y_r^{III} max\{0,\ \omega_i^y - t_r\}\right) \tag{63}$$

5.3. Overall formulation of the TNC's problem

The overall problem encompassing MARUE (section 4) and the TNC's decisions (section 5) has a bi-level structure and is integrated into an MPCC shown in P3. The objective function of the MPCC describes TNC profit maximization, while complementarity constraints (2) and (31) and logit mode choice constraints (55) and (64), along with other constraints, capture traveler section/route and mode choice under equilibrium. Thus, on the one hand, the TNC maximizes its profit anticipating traveler choice; on the other hand, traveler choices are made given the TNC fleet size, fare, and vehicle routing and state allocation decisions.

Note that for computational convenience, we transform the logit function (38) to an equivalent one-dimensional function using Eqs. (55) and (64). All sgn, max, and min functions are approximated by continuous functions following Eqs. (45)-(47).

(P3): MPCC-TNC

$$\left(\begin{array}{c} max \\ {\scriptstyle F,\ \boldsymbol{f},\ \boldsymbol{y},} \\ {\scriptstyle \boldsymbol{q},\ \boldsymbol{\eta},\ \boldsymbol{x},\boldsymbol{Q},\boldsymbol{H},\ \boldsymbol{C}} \end{array}\right) \tag{56}$$

s.t.

TNC's constraints (57)-(63)

Complementarity constraints (2), (25), and (31)

Flow and demand conservation constraints (3), (32), and (55)

$$\ln Q_{ij}^{m} - \ln Q_{ij}^{m'} = \varphi\left(U_{ij}^{m'} - U_{ij}^{m}\right), \forall (i,j) \in \Omega; m, m' \in M | m \neq m' \tag{64}$$

and definitional constraints of problem (P1)

The interactions among the major components of the MPCC-TNC model (P3) are summarized in Fig. 3. The blue arrows on the right represent the overarching bi-level structure of the model, which characterizes the interactions between the TNC (leader) and travelers (followers). The red arrows specify the coupling between network congestion and the decisions of the TNC and SAV/HV travelers. Specifically, SAV and HV flows (y_r^s and x_{ai}) contribute to network congestion (the thick red arrows toward "Road network congestion"). For HVs, the resulting link travel times (t_a) will adjust HV flows based on the user equilibrium principle (the thick red arrow toward "HV travelers' route choice"). TNC decisions on SAV flows, fleet size, and fare are made through maximizing profit, which is a function of route travel time (t_r), SAV waiting time in matching (ω_i^y), and SAV parking search time (PT_i), the latter two influenced by t_r (the orange arrow). Network travel times also influence SAV/HV travel costs and consequently traveler mode and section/route decisions (the red arrows toward "Travelers' (followers') decisions"). The green arrows highlight the coupling between the TNC decisions on SAV flows and the SAV traveler mode and section choices, through waiting times. The two thick green arrows toward "Waiting times" show that SAV flows (y_r^s) and SAV traveler flows (q_l) affect SAV/SAV traveler waiting times. In turn, SAV waiting times (ω_i^y) and consequent parking search time (PT_i) affect SAV flows (upward green arrow), and SAV traveler waiting times ($\omega_i^q, \varpi_i, \eta_l$) affect SAV traveler mode and section choice (downward green arrows toward "SAV travelers' section choice").

6. Solution method

We use the active set algorithm Lawphongpanich and Yin 2010) to solve P3. The basic idea is to sequentially solve a restricted problem of P3 where its complementarity constraints are replaced by regular (in)equality constraints. For notational simplicity, we hereafter use $\rho_{q,l}$, $\rho_{\eta,l}$, and $\rho_{x,ai}$ to represent the terms paired with variables q_l, η_l, and x_{ai} in the complementarity constraints (2), (25), and (31). We start by defining a pair of active sets $\Gamma_{(.)}$ and $\Gamma_{\rho_{(.)}}$ for each group of the above complementarity constraints, as in Eqs. (65)-(67). Note that the intersection of each active set pair (e.g., $\Gamma_q \cap \Gamma_{\rho_q}$) is not necessarily empty since strict complementarity is not required in (2), (25), and (31).

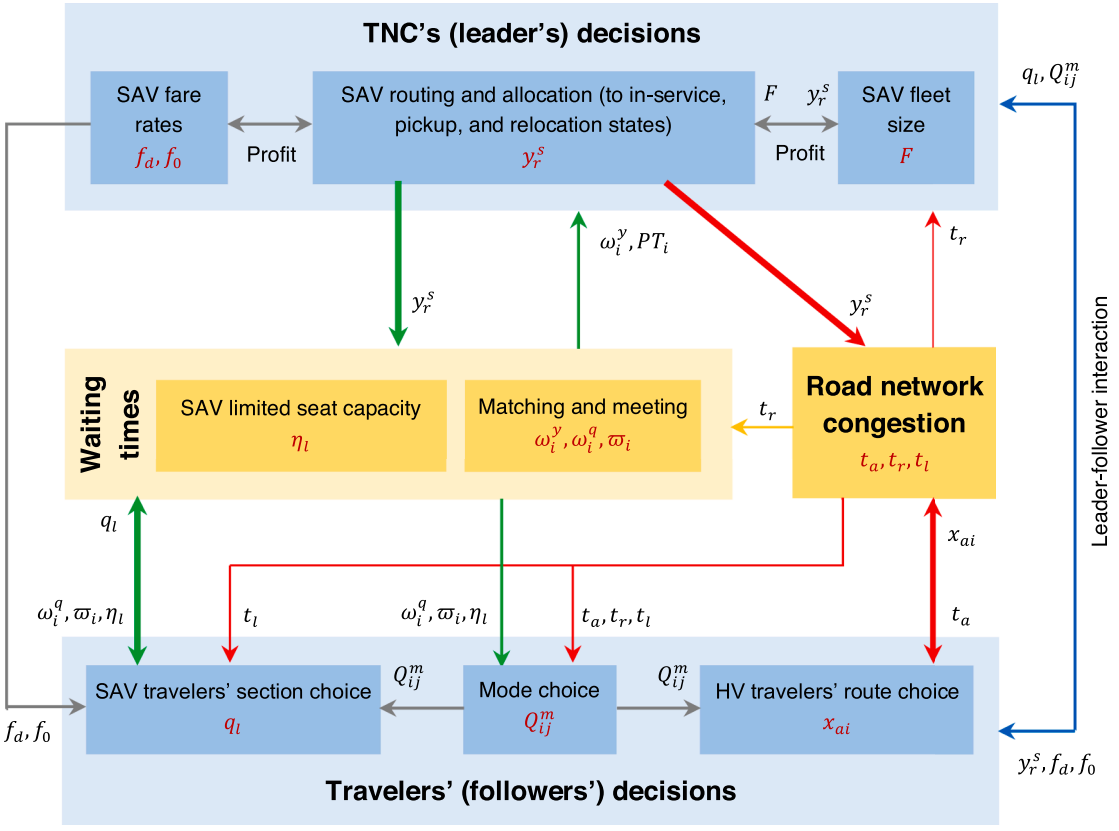

Fig. 3. Interactions of the major model components.

$$\Gamma_q = \{l \in L:\ q_l = 0\}, \Gamma_{\rho_q} = \{l \in L:\ \rho_{q,l} = 0\} \tag{65}$$

$$\Gamma_\eta = \{l \in L:\ \eta_l = 0\}, \Gamma_{\rho_\eta} = \{l \in L:\ \rho_{\eta,l} = 0\} \tag{66}$$

$$\Gamma_x = \{(a,i) \in A \times Z:\ x_{ai} = 0\}, \Gamma_{\rho_x} = \{(a,i) \in A \times Z:\ \rho_{x,ai} = 0\} \tag{67}$$

Given the active sets, we consider the following nonlinear program P4 termed NLP-TNC. Compared to P3, the complementarity constraints (2), (25), and (31) are replaced by regular (in)equality constraints (68)-(73) using the defined active sets.

(P4): NLP-TNC

$$\begin{pmatrix} max \\ F,f,y, \\ q,\eta,x,Q,H,C \end{pmatrix} \tag{56}$$

s.t.

TNC's constraints (57)-(63)

Flow and demand conservation constraints (3), (32), and (55)

Market share constraint (64)

Definitional constraints in P1

$$\begin{cases} q_l = 0 & \forall l \in \Gamma_q \\ q_l \geq 0 & \forall l \notin \Gamma_q \end{cases} \tag{68}$$

$$\begin{cases} \rho_{q,l} = 0 & \forall l \in \Gamma_{\rho_q} \\ \rho_{q,l} \geq 0 & \forall l \notin \Gamma_{\rho_q} \end{cases} \tag{69}$$

$$\begin{cases} \eta_l = 0 & \forall l \in \Gamma_\eta \\ \eta_l \geq 0 & \forall l \notin \Gamma_\eta \end{cases} \tag{70}$$

$$\begin{cases} \rho_{\eta,l} = 0 & \forall l \in \Gamma_{\rho_\eta} \\ \rho_{\eta,l} \geq 0 & \forall l \notin \Gamma_{\rho_\eta} \end{cases} \tag{71}$$

$$\begin{cases} x_{ai} = 0 & \forall (a,i) \in \Gamma_x \\ x_{ai} \geq 0 & \forall (a,i) \notin \Gamma_x \end{cases} \tag{72}$$

$$\begin{cases} \rho_{x,ai} = 0 & \forall (a,i) \in \Gamma_{\rho_x} \\ \rho_{x,ai} \geq 0 & \forall (a,i) \notin \Gamma_{\rho_x} \end{cases} \tag{73}$$

The active set algorithm proceeds as follows.

Step 1: Initialize. Find a feasible solution ($\boldsymbol{F}$, $\boldsymbol{f}$, $\boldsymbol{y}$, $\boldsymbol{q}$, $\boldsymbol{\eta}$, $\boldsymbol{x}$, $\boldsymbol{Q}$, $\boldsymbol{H}$, $\boldsymbol{C}$) to P3. Set iteration counter $k = 1$ and construct active sets $\Gamma^k_{(.)}$ and $\Gamma^k_{\rho_{(.)}}$ as defined in Eqs. (65)-(67) based on the feasible solution.

Step 2: Solve P4. Set $\Gamma_{(.)} = \Gamma^k_{(.)}$ and $\Gamma_{\rho_{(.)}} = \Gamma^k_{\rho_{(.)}}$ in Eqs. (65)-(67). Solve P4 to obtain ($\boldsymbol{F}^k$, $\boldsymbol{f}^k$, $\boldsymbol{y}^k$, $\boldsymbol{q}^k$, $\boldsymbol{\eta}^k$, $\boldsymbol{x}^k$, $\boldsymbol{Q}^k$, $\boldsymbol{H}^k$, $\boldsymbol{C}^k$). Because the active sets are given which satisfy the complementarity constraints (2), (25), and (31), P4 is a restricted problem of the original problem P3.

Step 3: Check convergence. Denote the Lagrange multipliers of the equality constraints in (68)-(73) by $\psi_{q,\ l}$, $\psi_{\rho_q,l}$, $\psi_{\eta,\ l}$, $\psi_{\rho_\eta,l}$, $\psi_{x,ai}$, $\psi_{\rho_x,ai}$. Construct new pairs of sets $\Psi_{(.)}$ and $\Psi_{\rho_{(.)}}$ as follows.

$$\Psi^k_q = \left\{l \in \left(\Gamma^k_q \cap \Gamma^k_{\rho_q}\right) : \psi_{q,l} > 0\right\}, \Psi^k_{\rho_q} = \left\{l \in \left(\Gamma^k_q \cap \Gamma^k_{\rho_q}\right) : \psi_{\rho_q,l} > 0\right\}; \Psi^k_\eta = \left\{l \in \left(\Gamma^k_\eta \cap \Gamma^k_{\rho_\eta}\right) : \psi_{\eta,l} > 0\right\},$$
$$\Psi^k_{\rho_\eta} = \left\{l \in \left(\Gamma^k_\eta \cap \Gamma^k_{\rho_\eta}\right) : \psi_{\rho_\eta,l} > 0\right\}; \Psi^k_x = \left\{(a,i) \in \left(\Gamma^k_x \cap \Gamma^k_{\rho_x}\right) : \psi_{x,ai} > 0\right\}, \Psi^k_{\rho_x} = \left\{(a,i) \in \left(\Gamma^k_x \cap \Gamma^k_{\rho_x}\right) : \psi_{\rho_x,ai} > 0\right\}$$

If $\Psi^k_q = \Psi^k_{\rho_q} = \Psi^k_\eta = \Psi^k_{\rho_\eta} = \Psi^k_x = \Psi^k_{\rho_x} = \varnothing$, stop and ($\boldsymbol{F}^k$, $\boldsymbol{f}^k$, $\boldsymbol{y}^k$, $\boldsymbol{q}^k$, $\boldsymbol{\eta}^k$, $\boldsymbol{x}^k$, $\boldsymbol{Q}^k$, $\boldsymbol{H}^k$, $\boldsymbol{C}^k$) is the strongly stationary solution of P3. Otherwise, go to Step 4.

Step 4: Update active sets. For each pair of active sets $\Gamma_{(.)}$ and $\Gamma_{\rho_{(.)}}$ in Eqs. (65)-(67), do the following:

If $\Psi^k_{(.)} \cap \Psi^k_{\rho_{(.)}} = \varnothing$, then set $\Gamma^{k+1}_{(.)} = \Gamma^k_{(.)} - \Psi^k_{(.)}$ and $\Gamma^{k+1}_{\rho_{(.)}} = \Gamma^k_{\rho_{(.)}} - \Psi^k_{\rho_{(.)}}$ Else

For each $l \in \Psi^k_{(.)} \cap \Psi^k_{\rho_{(.)}}$ If $\psi_{(.),\ l} > \psi_{\rho_{(.)},l}$, then $\Psi^k_{\rho_{(.)}} = \Psi^k_{\rho_{(.)}} - l$Else $\Psi^k_{(.)} = \Psi^k_{(.)} - l$End If

End For

Set $\Gamma^{k+1}_{(.)} = \Gamma^k_{(.)} - \Psi^k_{(.)}$ and $\Gamma^{k+1}_{\rho_{(.)}} = \Gamma^k_{\rho_{(.)}} - \Psi^k_{\rho_{(.)}}$ End If

Set $k = k + 1$ and go back to Step 2.

In the algorithm, step 1 requires an initial feasible solution to P3. The initial solution is found by solving an equivalent NLP of P2

using a primal-dual gap function (see Appendix 2), provided a feasible decision (including f_0, f_d, and y_r^s, $r \in R$, $s \in S$) for the TNC. For the feasible decision for the TNC, arbitrary values are given to f_0 and f_d. For y_r^s, we fix the SAV relocation flows to zero, and equally assign all in-service and pickup SAVs to the shortest-distance route for each OD, so that a given SAV traveler demand (as an arbitrary portion of total demand) for each OD is satisfied assuming that each SAV takes one traveler.

7. Numerical analysis

We implement the model in the Sioux Falls network (Fig. 4) to investigate the system performance with coexisting SAVs and HVs. Several interesting results are presented, including the baseline scenario (section 7.1) and scenario analysis of the effects of SAV ridesharing, SAV relocation, SAV size, matching elasticity, SAV price, and in-vehicle VOT saving of SAV travelers (section 7.2). The results are also compared to a present-day scenario with only HVs (i.e., $Q_{ij} = Q_{ij}^{HV}, \forall (i,j) \in \Omega$).

The road network has 76 links and 24 nodes, of which 12 represent zones (in total 132 OD pairs). Link characteristics, such as free-flow travel time ($t_{0,a}$) and base capacity (K_a^{HV}), are borrowed from Transportation Test Networks (2017). The demand matrix (Q_{ij}) in Transportation Test Networks (2017) is scaled up such that the total trip generation from each of the 12 zones becomes similar to that of the original demand matrix. We create 2742 routes for SAVs (including 12 virtual intra-zone routes with zero costs) and 1704 sections for SAV travelers using Yen's k-shortest path algorithm (Yen 1971). Specifically, for each OD pair we identify up to 30 shortest-distance routes with the route length constrained to be no more than three times the length of the shortest-distance route. A similar procedure is implemented to identify sections (see Appendix 3 for step-by-step construction of sections). For HV travelers, route enumeration is not needed as we employ a link-node formulation (see section 4.2).

The model and the active set algorithm are coded in GAMS and solved using the generalized reduced gradient algorithm of CONOPT on a computer with Intel/Core i7 3.20 GHz with 16 GB RAM. The MPCC (P3) has 74,369 variables and 70,433 constraints, of which 4320 are complementarity constraints. The average (respectively, standard deviation) of the number of iterations and the solution time (in minutes) of the active set algorithm over the 21 scenarios implemented in this section are respectively 8.4 (4.0) and 19.6 (5.7), of which 3.3 (1.5) minutes are spent in finding initial feasible solutions (step 1 of the active set algorithm). For the present-day scenario with only HVs, we solve an equivalent NLP to P1 (the NLP will be formed in a similar way as P5 in Appendix 2) using CONOPT, which takes 4.1 s.

7.1. Baseline scenario

The baseline is set up with 4-seat sedan SAV/HV with main modeling parameters listed in Table 2. Note that κ denotes the seat capacity of an SAV (and also an HV), not occupancy. For an HV, only one seat will be occupied. We assume that SAV price is 20% higher

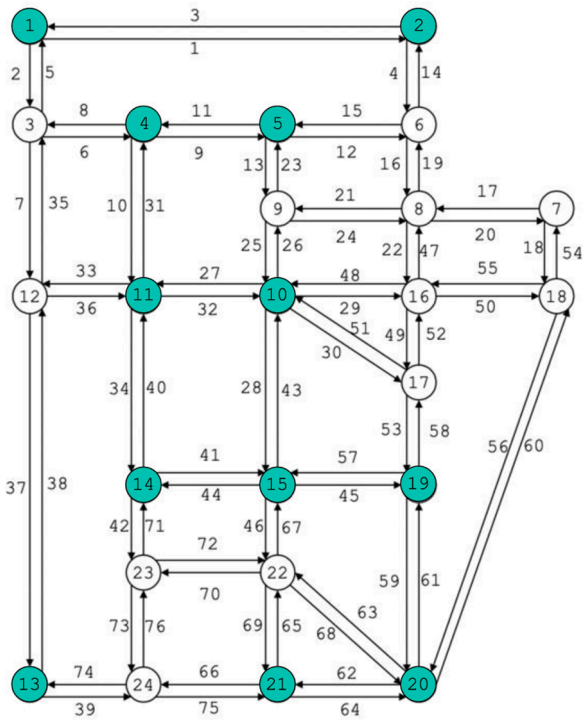

Fig. 4. The Sioux Falls road network (Note: colored nodes also represent zones).

Table 2
Main modeling parameters.

Vehicle type(body size)	Vehicle attributes			Traveler attributes	
	Price ($k)	Variable cost ($/mi)	Headway (*sec*)	In-vehicle VOT ($/hr)	Waiting VOT ($/hr)
HV (4-seat sedan)	35	0.25	1.6	14.2	14.2
SAV (4-seat sedan)	42 (20% ↑)	0.28	0.6	11.4 (20% ↓)	14.2

than that of HV to reflect the self-driving technology cost Bösch et al., 2018). The distance-based vehicle operating cost is calculated as the sum of the fixed cost (due to depreciation of vehicle price) and the variable cost (due to insurance, fuel, and maintenance). The fixed cost θ_1^m is derived by assuming an average annual VMT at 15,000, 10% annual depreciation rate for HVs (Bösch et al., 2018) over a 5-year vehicle lifetime (AAA 2015), and 40% annual depreciation rate for SAVs (Bizfluent 2017). The variable cost θ_2^m is computed based on an annual variable cost of $3750 for HVs (AAA 2015), which is modified for SAVs assuming 30% insurance discount, 10% fuel efficiency, and an additional $1000/year in maintenance cost due to self-driving technology. For SAVs, the time-based fixed ownership cost (μ) equals $4.6/hour assuming the 40% annual depreciation rate and a 10-hour daily service time. We follow Nowakowski et al. (2010) and assume vehicle headways at capacity (τ_m) of 1.6 and 0.6 s for HVs and SAVs. We assume 20% saving in in-vehicle VOT (γ_2^m) for SAV users compared to that for HV users, which is $14.2/hour (USDOT 2016). Waiting VOT (γ_1) is also set at $14.2/hour. The logit scale factor (φ) is set to 0.5. Following Yang and Yang (2011), the matching function parameters in Eq. (12) are $B_i = 0.25$ and $b_1 = b_2 = 0.75$. $b_1 + b_2 > 1$ suggests increasing returns-to-scale of matching. The free-flow parking search time in each zone ($PT_{0,i}$) and parking search speed ($\mathcal{S}_i$) are 0.1 hr (Lam et al., 2006) and 7 mi/hr (Belloche 2015). To prevent illegal parking, the zonal parking capacity (PK_i) equates the hourly demand destined to a zone. We consider the parameters of the BPR functions in Eqs. (35) and ((42) to be $\alpha_a = 0.15$, $\beta_a = 4$ and $\alpha_i = 0.3$, $\beta_i = 4$ (Lam et al., 2006).

Table 3 presents the baseline results. The TNC charges each SAV traveler a fixed amount of $3.32/ride plus $0.30/mile and earns about $216k in profit in a one-hour period. The optimal SAV fleet size is 11,059 which equals 5.7% of the total hourly travel demand (i.e., $\sum_{(i,j)\in\Omega} Q_{ij}$). The fleet utilization — which measures the percent time an SAV is in the in-service state ($s = I$), calculated as $\sum_{r\in R} y_r^I t_r / F$ based on Eq. (63) — is 40%. We find that the SAV hours spent in the pickup state ($s = II$) significantly outnumbers that of the relocation state ($s = III$). The systemwide market shares of SAV and HV, calculated as $100 \times \sum_{(i,j)\in\Omega} Q_{ij}^m / \sum_{(i,j)\in\Omega} Q_{ij}, (\forall m \in M)$, are 35% and 65%. The average occupancy of an SAV — which is a weighted average of $(q_l + \tilde{q}_l)/\pi_l$ based on Eq. (25) over all sections l with $\pi_l \neq 0$, weighted by SAV traveler flow $(q_l + \tilde{q}_l)$ — is 3.45 travelers. The average traveler group size — which is a weighted average of σ_i^q over all zones, weighted by the SAV traveler flow originating from each zone n_i^q — is 2.71. Also, out of the 12 zones, only one zone has unmatched SAVs (which occurs when $\overline{n}_i^y > n_i^y$). The average matching times of an SAV and an SAV traveler are 11.9 and 2.4 min, respectively.

In the last column of Table 3, we also compare the baseline to the present-day scenario with only HVs. We find that each SAV replaces 6.2 HVs, which is the ratio of SAV traveler demand to the SAV fleet size, assuming that each unit of travel demand would require one HV if SAVs were absent. As a result of the replacement, occupied VMT is significantly reduced (by 20%). Enabled by ridesharing, the total VMT is also reduced (by 18%) despite empty SAV trips. The reduction in total VMT and 17% increase in network capacity alleviate congestion, which leads to 15% decline in total traveler en-route time. Due to in-vehicle VOT saving of SAV travelers and ridesharing, SAVs reduce the total generalized travel cost by 31%.

Fig. 5 illustrates how travelers of multiple ODs share SAVs, using two SAV routes r_1 (starting at zone 15 and ending at zone 1) and r_2 (starting at zone 10 and ending at zone 13). The SAV route flows ($y_{r_1}^I$ and $y_{r_2}^I$, in SAVs/hour), travel times (both under congestion and free flow) on each route and the component links, and SAV traveler flows of all sections using each route ($q_{lr}, l = 1, \ldots, 13; r = 1, 2$, in travelers/hour) are also reported. SAV route r_1 serves SAV travelers of 10 sections. Of the total 516.8 (129.2 × 4) SAV seats on route r_1, 40% (208.0 / 516.8) are occupied throughout r_1 by travelers of section l_1, who have the same OD as r_1. The remaining SAV seats are used either by travelers who are picked up at the origin of r_1 and dropped off before the route ends (sections l_2, l_3, and l_4), or by travelers who are picked up en route on r_1 (sections l_5, l_6, l_7, l_8, l_9, and l_{10}). It can be easily verified that SAVs on route r_1 are fully occupied in the portion between zones 15 and 14, as the sum of SAV traveler flows of sections l_1, l_2, l_3, and l_4 equals the SAV seats on the

Table 3
Baseline results.

TNC		Travelers		Change in system performance*	
Constant fare ($/ride)	3.32	Market share (%)		SAV-HV replacement ratio	6.2
Distance-based fare ($/mile)	0.30	SAV	35.3	Total traveler generalized cost	−31.4
Fleet size (% of total demand)	5.69	HV	64.7	Total traveler en-route time	−15.3
SAV hours in each state (%)		Avg. SAV occupancy	3.45	Total VMT	−17.8
In-service	40.4	Avg. SAV traveler group size	2.71	Occupied VMT	−20.0
Pickup	51.1	Avg. matching time (min)	2.4	Road network capacity	16.8
Relocation	8.5				
Profit ($k)	215.7				
Avg. matching time (min)	11.9				

* Compared to the present-day scenario with only HVs.

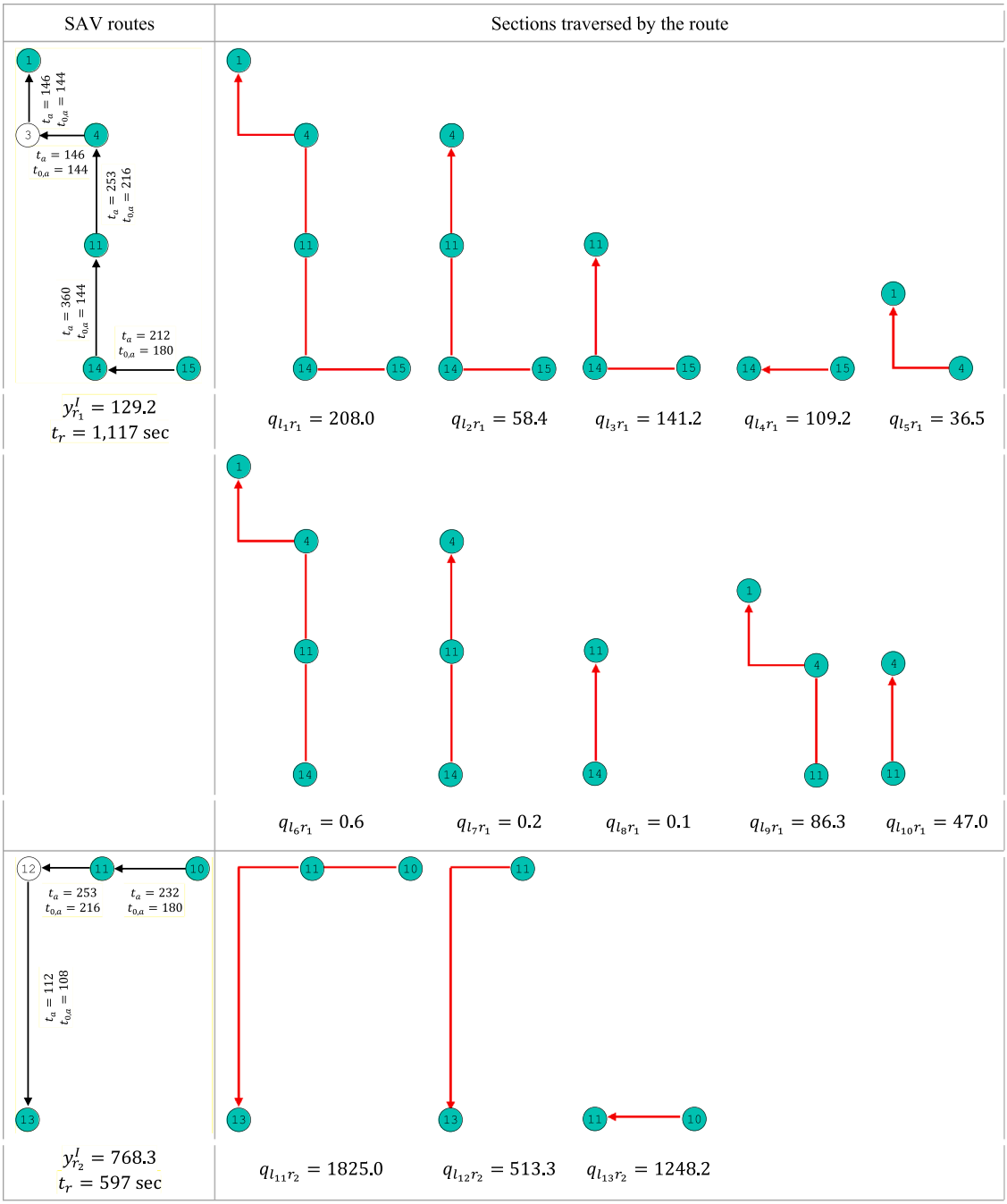

Fig. 5. Illustration of how travelers of multiple ODs share SAVs in the baseline scenario.

route. Similar analysis can be done for SAV route r_2.

7.2. Scenario analysis

This section further investigates how system performance will change without ridesharing or automation or relocation, and if we consider alternative SAV (body) sizes, matching elasticities, SAV prices, and in-vehicle VOT savings for SAV travelers. The results are compared with the baseline and present-day (HV-only) scenarios.

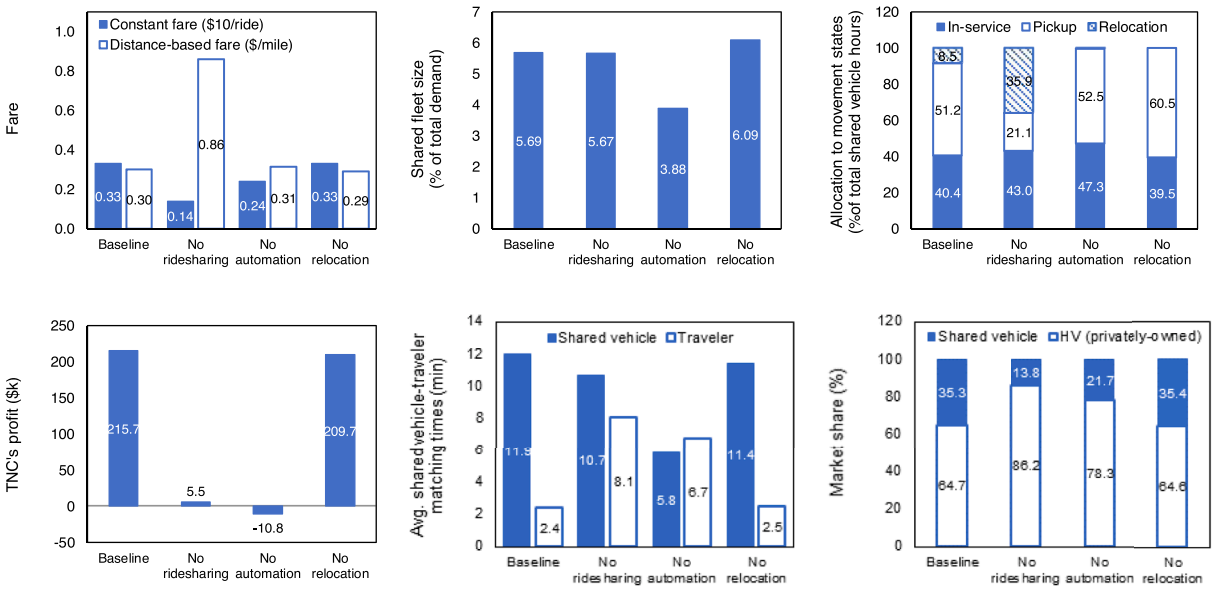

Fig. 6. Changes in system performance compared to the baseline scenario, without ridesharing, without automation, and without relocation.

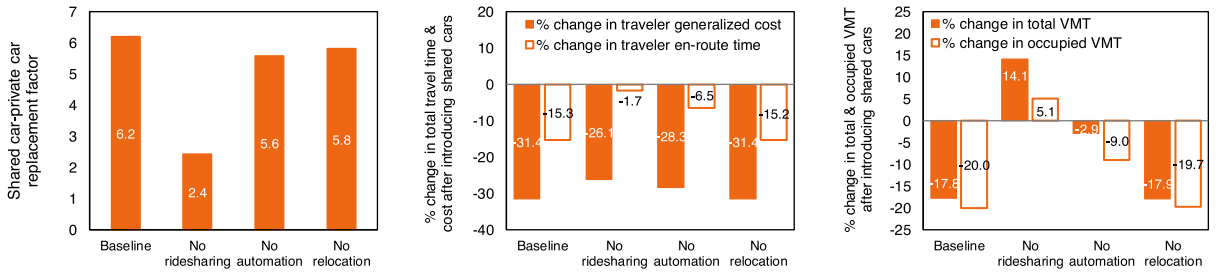

Fig. 7. Changes in system performance compared to the present-day scenario (only HVs), without ridesharing, without automation, and without relocation.

7.2.1. No ridesharing

When ridesharing is not allowed, an SAV has at most one traveler at any time. Figs. 6 and 7 present the results. The system performance is drastically worse off than the baseline in terms of TNC profit, traveler en-route time, generalized travel cost, and total and occupied VMT. Particularly, the total and occupied VMT will even worse off the present-day (HV-only) scenario. This is not surprising as the SAV fleet size remains almost the same as the baseline but each single-occupancy SAV replaces only 2.4 HVs (compared to 6.2 under the baseline) and empty SAV relocation miles is quadrupled. The SAV market share drops from 35% under the baseline to 14% due to the aggravated system performance and increased fare and matching time. For SAV fare, while the constant fare per ride is almost halved, the distance-based fare is tripled. The matching time of SAV travelers is increased by more than 300%. By contrast, the change in the matching time of SAVs is much smaller, with a marginal reduction by about 10%.

7.2.2. No automation

Without vehicle automation, we assume that the TNC owns a fleet of shared HVs operated by salaried drivers who fully comply with the TNC's recommendations for vehicle allocation, relocation, and routing. Different from the baseline scenario, the TNC pays $35k for purchasing each HV and $13/hour for drivers' salaries (Indeed, 2021), can use only three of the vehicle seats due to the presence of a driver, and cannot enjoy reduced vehicle headways. As a result, the time-based fixed ownership cost (μ) increases from $4.6/hour in the baseline scenario to $16.8/hour ($13/hour for driver salary plus $3.8/hour for vehicle depreciation assuming a 40% annual depreciation rate and a 10-hour daily service time similar to the baseline) and the variable operating cost reduces from $0.28/mile in the baseline to $0.25/mile similar to that of private HVs (Table 2). Note that this kind of HV ridesharing is different from the prevalent Uber-like HV ridesharing (i.e., drivers own their HVs and can decide when to start and end service (resulting in a varying fleet size) and whether to follow the TNC's recommendations on rider pickup or relocation) and self-organized non-profit HV ridesharing (e.g., those studies in Table 1).

As shown in Figs. 6 and 7, the system performance is degraded relative to the baseline scenario in terms of TNC profit, traveler en-route time, generalized travel cost, and total and occupied VMT. Due to a higher time-based fixed vehicle ownership cost, reduced vehicle seat capacity (with a driver inside), and no congestion mitigation benefits from vehicle headway reduction, the TNC profit will turn negative. The TNC actually will reduce its fleet size from 5.7% (baseline) to 3.9% of the total demand. Compared to the baseline, the traveler matching time will increase by 280% and the TNC will lose nearly 14% of its market share, despite reduced constant fare and almost unchanged distanced-based fare.

7.2.3. No relocation

Without relocation, an SAV must stay at the zone where its previous in-service state ended, waiting to be matched with future traveler(s) from any zone and then moving unoccupied to that zone to pick up the matched traveler(s). The results (Fig. 6-7) indicate only a marginal deterioration in system performance compared to the baseline in terms of TNC profit, traveler en-route time, generalized travel cost, and total and occupied VMT. This is not surprising by noting that SAVs spend only 8% of their time for relocation in the baseline, and that the purpose of relocation (i.e., reducing traveler waiting time by proactively dispatching SAVs before demand arises) can be partly satisfied by ridesharing since it enables in-service SAVs to pick up waiting travelers while en route and thus reduce traveler waiting times. This is evidenced by matching times being close to the baseline. The SAV market share is similar to the baseline as the TNC compensates for the marginal system performance degradation by marginally increasing the SAV fleet size (from 5.7% in the baseline to 6.1%) and keeping SAV fare unchanged.

7.2.4. SAV size

The baseline considers 4-seat sedan SAVs at the price of $42k. To understand the effect of SAV (body) size, two alternative scenarios with different SAV sizes are investigated: 1-seat solo SAVs and 8-seat van SAVs. Their prices are assumed $13k and $66k respectively, following Bösch et al. (2018) plus a 20% markup to reflect the self-driving technology cost. The time-based fixed ownership cost (μ) of solo and van SAVs are calculated in a similar way to that of sedan SAV in the baseline. The variable costs are calculated by scaling that of sedan SAV, according to Table B.1 in Bösch et al. (2018). Figs. 8 and 9 present the results.

The results show clear economies of SAV size. More specifically, using larger SAVs will increase TNC profit and reduce traveler en-route time, generalized travel cost, and total and occupied VMT. This is because more travelers can be accommodated in larger SAVs, which contributes to reducing the number of required SAVs to meet demand, SAV relocation hours, and the occupied and total VMT. However, the economies of SAV size diminishes as we increase SAV size from solo to sedan to van, as reflected in the extent of change in TNC profit, SAV market share, and SAV/traveler matching times.

7.2.5. Matching elasticity

Recall from Eq. (12) that b_1 and b_2 are the matching elasticities with respect to SAV traveler demand and SAV supply. Values for the two parameters reflect the efficiency of the matching algorithm in the TNC's online platform used by SAV travelers. Larger b_1 and b_2 imply more efficient matching. We rerun the model with b_1 and b_2 taking values from 0.5 to 1 in 0.1 intervals. Figs. 10 and 11 demonstrate the results.

With increased b_1 and b_2, SAV and traveler matching times will decrease as expected. The matching efficiency improvement also leads to a smaller SAV fleet size to meet a greater SAV market share, thus yielding a higher TNC profit. However, SAV market share

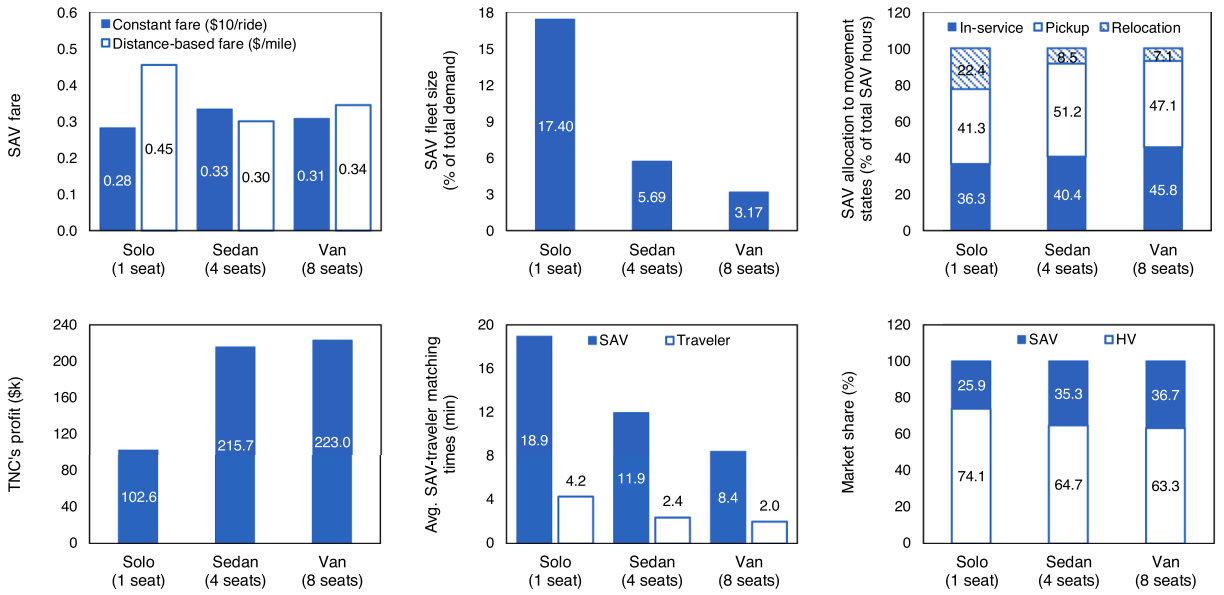

Fig. 8. Changes in system performance compared to the baseline scenario, with different SAV sizes.

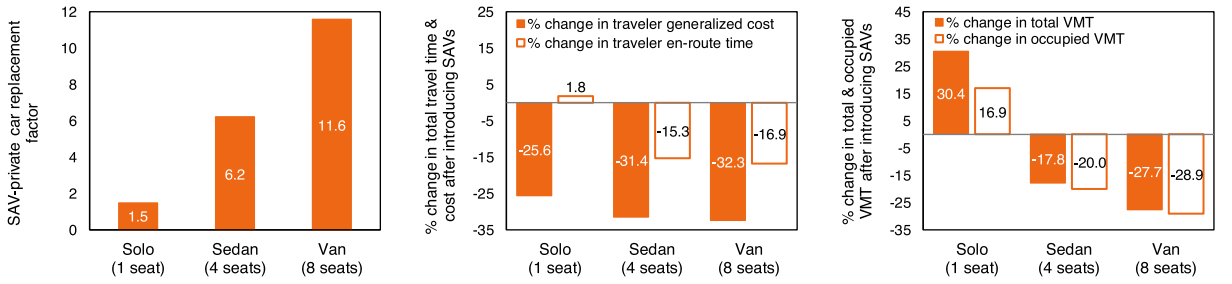

Fig. 9. Changes in system performance compared to the present-day scenario (only HVs), with different SAV sizes.

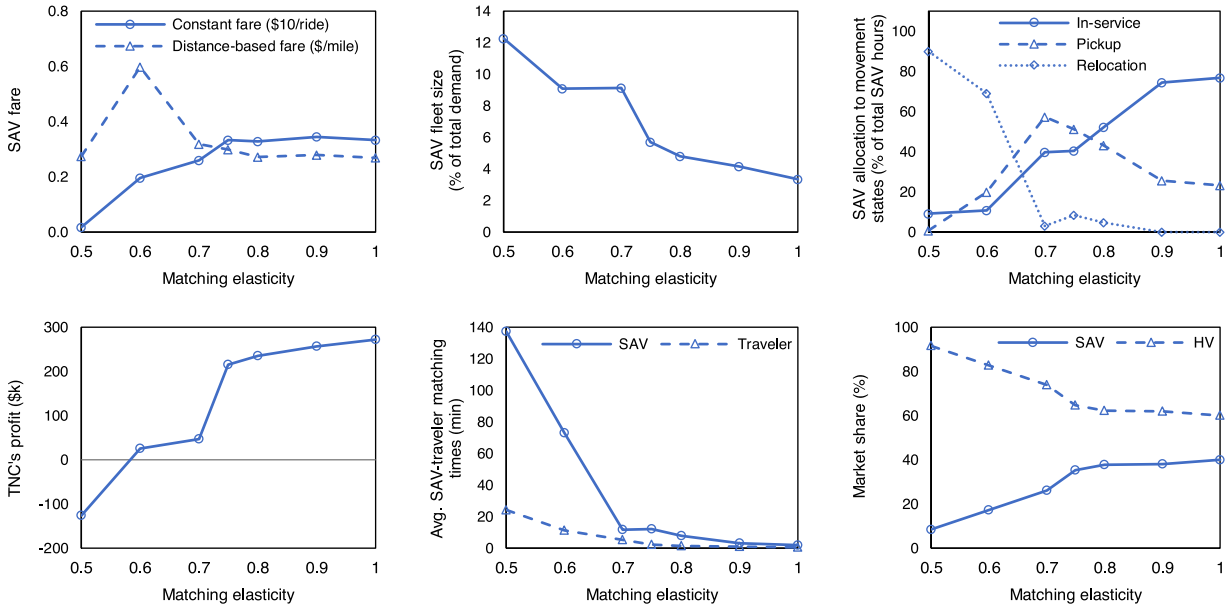

Fig. 10. Impact of matching elasticity on system performance compared to the baseline scenario.

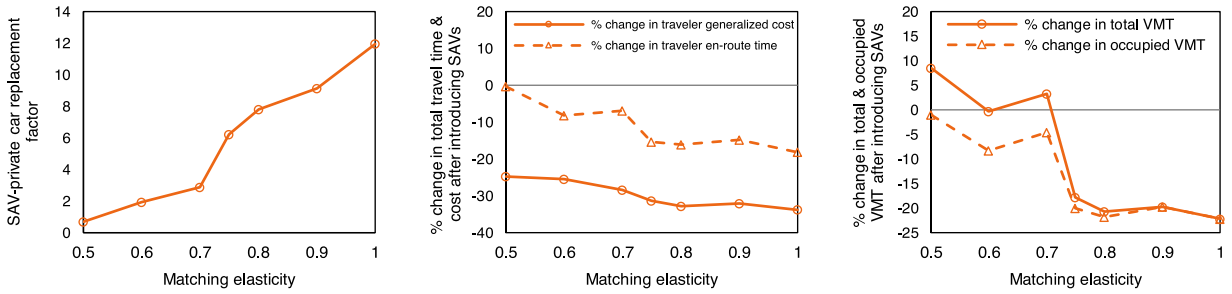

Fig. 11. Impact of matching elasticity on system performance compared to the present-day scenario (only HVs).

appears to be "capped" when the matching elasticity is above 0.75. The changes in total and occupied VMT, en-route travel time, and generalized travel costs compared are not monotonic with respect to matching efficiency, which are associated with fluctuations in relocating SAV hours as we increase matching efficiency.

7.2.6. SAV price

The price markup of SAVs is expected to drop with technological development and industrial scale production. This section varies the SAV price markup from 0% to 100% of the HV price in 20% increments, to understand the impact on the TNC, travelers, and system performance. Figs. 12 and 13 exhibit the results. Interestingly, we find that the SAV market share remains largely constant for the range of SAV price considered. This may be attributed to the overall conflicting trends in distance-based and constant fare rates as well as the

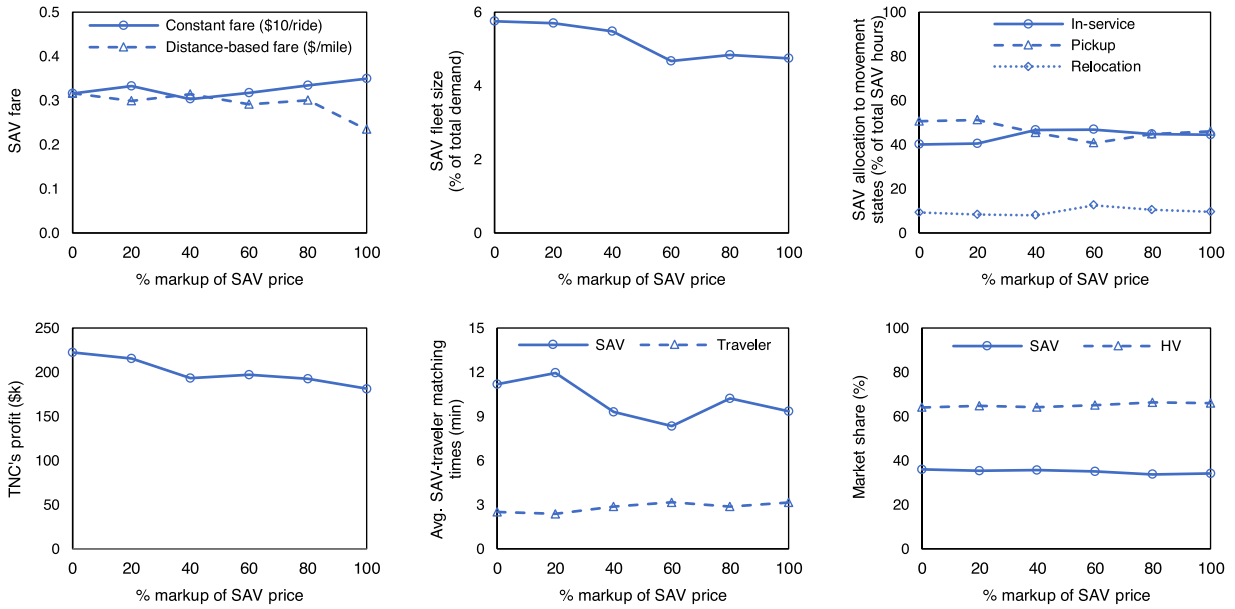

Fig. 12. Impact of SAV price on system performance compared to the baseline scenario.

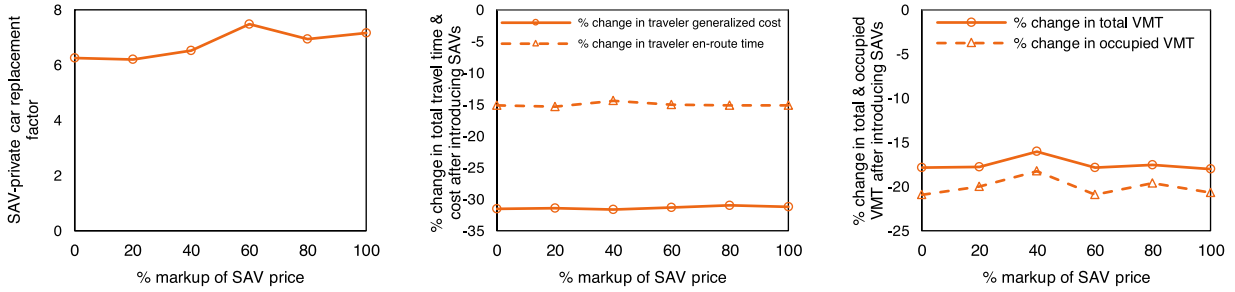

Fig. 13. Impact of SAV price on system performance compared to the present-day scenario (only HVs).

overall unchanged traveler matching times, which do not affect the attractiveness of SAV. Moderately nonmonotonic changing trends are observed for other aspects of system performance, including TNC profit, SAV fleet size, SAV-HV replacement ratio, and changes in traveler en-route time, generalized travel cost, and total and occupied VMT.

7.2.7. In-vehicle VOT saving

In-vehicle VOT saving is a major benefit of using SAVs. However, the exact extent of saving is unclear. In this section, we examine the impact of in-vehicle VOT saving on the TNC, travelers, and system performance by changing it from 0 to 50% in 10% intervals. Figs. 14 and 15 present the results. As expected, more travelers will use SAVs as in-vehicle VOT saving increases. The TNC's responses in distance-based and constant fare rates, which are nonmonotonic, counteract the benefit brought by a larger VOT saving. The nonmonotonic changing trends of SAV fare, fleet size, and allocation lead to similar variations in total and occupied VMT, total en-route travel time, and total generalized travel cost.

8. Conclusions

This paper makes a first attempt to model autonomous ridesharing — multiple travelers jointly riding one shared autonomous vehicle (SAV) — in a static network equilibrium setting with mixed SAV and human-driven vehicle (HV) traffic. Two methodological contributions are made, filling major gaps between network modeling of private and shared mobility. First, we propose a novel *one (SAV)-to-many (riders) matching* to characterize the SAV/riders waiting times during online matching. The proposed matching function accommodates the possibilities of a traveler matched with an SAV starting from the same origin, whereto the SAV moved unoccupied in either pickup or relocation state, or with an en-route SAV that goes through the traveler's origin in the in-service state and does not incur stopping other than picking up the traveler. Second, we introduce a section-based formulation for SAV ridesharing equilibrium, in which the SAV traveler flow and SAV seat capacity utilization are characterized at the section level. The notion of section allows for

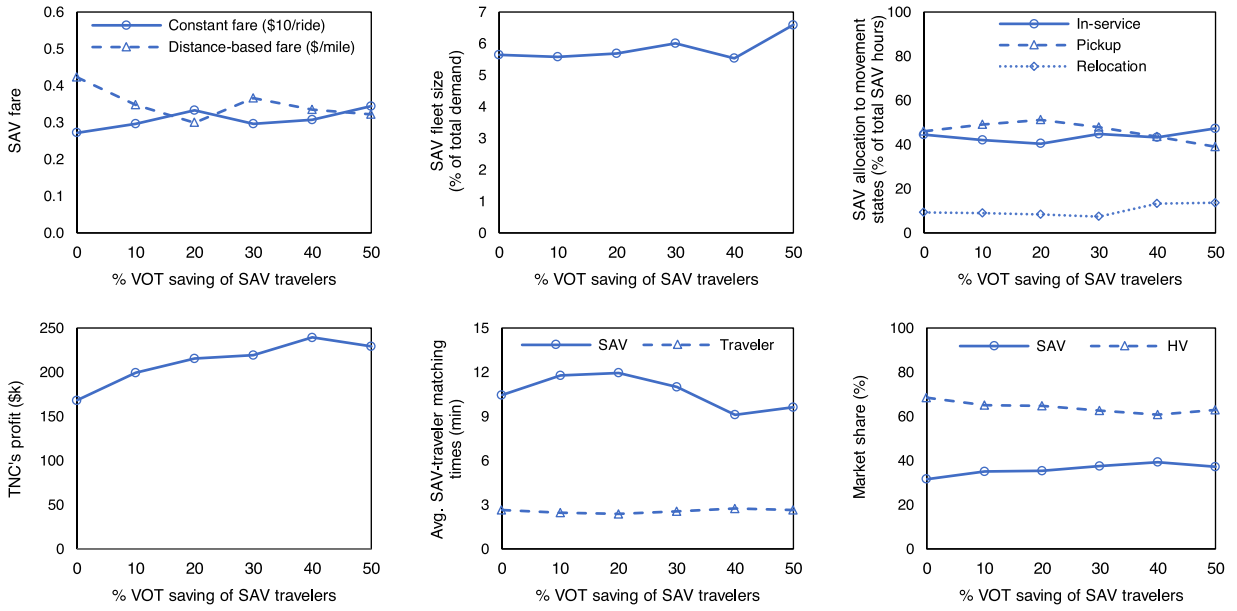

Fig. 14. Impact of in-vehicle VOT saving on system performance compared to the baseline scenario.

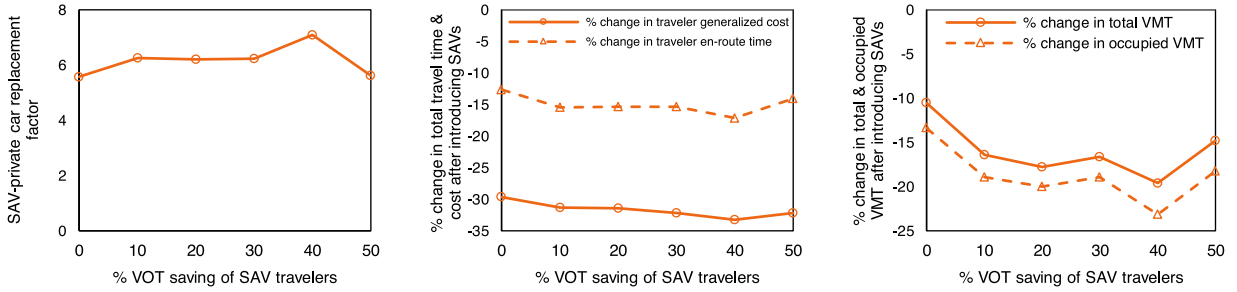

Fig. 15. Impact of in-vehicle VOT saving on system performance compared to the present-day scenario (only HVs).

consideration of dissimilar SAV/travelers itineraries (OD pairs) which is inherent in ridesharing, while preventing rider en-route transfer(s) in existing link-based ridesharing formulations.

To endogenously characterize the travel demand for coexisting SAV/HV, a new multimodal autonomous ridesharing user equilibrium (MARUE) is put forward with a proof of its existence. Building on MARUE, we also seek to determine the optimal supply decisions of a transportation network company comprising the *SAV fleet size, fare, routing, and allocation* (to the in-service, pickup, and relocation states). The overall TNC supply-traveler demand problem is formulated as a mathematical program with complementarity constraints and solved using the active set algorithm. We obtain several original insights through numerical analysis about the benefits SAV ridesharing brings to the overall system, the distribution of SAV hours in in-service, pickup, and relocation states, and diminishing economies of SAV (body) size.

Further research can be extended in a few directions. First, as this paper considers that SAV travelers on an OD can make choices among different sections, it would be useful to investigate an alternative situation that the TNC is responsible for allocating travelers to sections. Comparing system performance under the two situations can generate interesting insights about the effect of providing travelers with routing flexibility on future autonomous ridesharing. This investigation could be jointly undertaken considering multiple TNCs, presumably through formulating and solving an equilibrium problem with equilibrium constraints. An interesting scenario could be some TNCs running SAVs and some TNCs running HVs. Second, as enumeration of SAV routes and SAV traveler sections is needed in the current formulation, future research could explore methods such as column generation (He et al., 2014; Chen et al., 2016c) to more efficiently generate routes and sections. Third, besides waiting/matching time, further consideration of ridesharing inconvenience cost could be helpful. Inconvenience cost may include social and physiological/psychological aspects such as approval of strangers sharing the same vehicle (Liu and Li, 2017; Lavieri and Bhat, 2019; Clayton et al., 2020) and perceived security of SAVs (Merfeld et al., 2019; Li et al., 2020b), and can be considered as an increasing function of the vehicle occupancy (Di et al., 2018; Di and Ban 2019) or travel time during the shared ride (Ma et al., 2020).

Finally, while our focus is on one-to-many matching and section-based formulation of autonomous ridesharing with coexistence of

solo HVs, the presence of other types of vehicles and services could be jointly considered. For example, for-profit HV ridesharing like UberPool, for which we are not aware of any network equilibrium study, bears similarities with SAV service. Thus, the modeling could use/adapt many of the formulations and solution technique developed in the paper. On the other hand, however, by owning vehicles ridesharing drivers can decide when to start and end service (resulting in a varying fleet size) and whether to follow the TNC's recommendations on rider pickup or relocation. Another, more traditional service type is taxi without ridesharing, for which the modeling can follow established approaches (e.g., Wong et al., 2001; 2008). A third service type of interest is self-organized non-profit HV ridesharing, which involves citizen drivers sharing rides during their own trip (e.g., from home to work) in exchange for some compensation. For the self-organized nonprofit HV ridesharing, the methodologies developed in studies in Table 1 could be followed.

CRediT authorship contribution statement

Mohamadhossein Noruzoliaee: Conceptualization, Methodology, Formal analysis, Investigation, Writing – original draft, Writing – review & editing, Visualization. **Bo Zou:** Conceptualization, Methodology, Formal analysis, Investigation, Writing – original draft, Writing – review & editing, Supervision.

Acknowledgement

This research was funded in part by the US National Science Foundation (NSF 2112650). The opinions expressed are solely those of the authors, and do not necessarily represent those of NSF. The authors would like to thank Associate Editor Prof. Srinivas Peeta, the handling editorial board editor, and three anonymous reviewers for the constructive comments which helped us improve the presentation of the paper.

Appendix 1. Proofs of Propositions 1–4

Proof of Proposition 1. For ω_i^q, Recall that $n_i^q/\sigma_i^q = n_i^y$. We replace n_i^y by n_i^q/σ_i^q in Eq. (13) and obtain $\omega_i^q = (\kappa)^{-\frac{b_2}{b_1}}(\sigma_i^q)^{\frac{2b_2-1}{b_1}}\left[(B_i)^{-\frac{1}{b_1}}(n_i^q)^{\frac{1-b_1-b_2}{b_1}}(\omega_i^y)^{-\frac{b_2}{b_1}}\right]$. If $b_2 > 0.5$, $(\sigma_i^q)^{\frac{2b_2-1}{b_1}} \geq 1$ as $\sigma_i^q \geq 1$ and $b_1 > 0$. Thus holding n_i^q and ω_i^y constant, ω_i^q is non-decreasing with ridesharing vs. without ridesharing. As $\frac{2b_2-1}{b_1} > 0$, it is evident that ω_i^q becomes larger with larger σ_i^q, i.e., more intense ridesharing.

For ω_i^y, we again replace n_i^y by n_i^q/σ_i^q in Eq. (14) and obtain $\omega_i^y = (\kappa)^{-1}(\sigma_i^q)^{\frac{2b_2-1}{b_2}}\left[(B_i)^{-\frac{1}{b_2}}(n_i^q)^{\frac{1-b_1-b_2}{b_1}}(\omega_i^q)^{-\frac{b_1}{b_2}}\right]$. Holding n_i^q and ω_i^q constant, it is easy to see that similar conclusions can be reached for ω_i^y with respect to b_2 and σ_i^q. □

Proof of Proposition 2. As shown in the proof for Proposition 1, $\omega_i^q = (\kappa)^{-\frac{b_2}{b_1}}(\sigma_i^q)^{\frac{2b_2-1}{b_1}}\left[(B_i)^{-\frac{1}{b_1}}(n_i^q)^{\frac{1-b_1-b_2}{b_1}}(\omega_i^y)^{-\frac{b_2}{b_1}}\right]$. Holding σ_i^q and ω_i^y constant, decreasing returns-to-scale of the Cobb-Douglas matching function means $b_1 + b_2 < 1$. Thus $\frac{1-b_1-b_2}{b_1} > 0$. If the SAV traveler flow is greater than 1 ($n_i^q > 1$), it is clear that ω_i^q increases with n_i^q. The same can be said for $\omega_i^y = (\kappa)^{-1}(\sigma_i^q)^{\frac{2b_2-1}{b_2}}\left[(B_i)^{-\frac{1}{b_2}}(n_i^q)^{\frac{1-b_1-b_2}{b_1}}(\omega_i^q)^{-\frac{b_1}{b_2}}\right]$ holding σ_i^q and ω_i^q constant. □

Proof of Proposition 3. Since the feasible region Φ of the VI problem (P2) as defined in Eqs. (3), (32), and (52)-(55) is polyhedron, the VI has an equivalent KKT system, written as follows (see Proposition 1.2.1 in Facchinei and Pang (2003)).

$$h_l - H_{ij} - \xi_{q,l} = 0, \forall l \in L_{ij};\ (i,j) \in \Omega \tag{A.1}$$

$$(\kappa\pi_l - q_l - \widetilde{q}_l) - \xi_{\eta,l} = 0, \forall l \in L \tag{A.2}$$

$$c_a + C_{D(a),i} - C_{O(a),i} - \xi_{x,ai} = 0, \forall a \in A; i \in Z \tag{A.3}$$

$$\left(\gamma_1 PT_j + PC_j^m + \frac{1}{\varphi}\ln Q_{ij}^m\right) + C_{ij} + \vartheta_{ij} = 0, \forall (i,j) \in \Omega; m = HV \tag{A.4}$$

$$\frac{1}{\varphi}\ln Q_{ij}^m + H_{ij} + \vartheta_{ij} = 0, \forall (i,j) \in \Omega; m = SAV \tag{A.5}$$

$$0 \leq \xi_{q,l} \perp q_l \geq 0, \forall l \in L \tag{A.6}$$

$$0 \leq \xi_{\eta,l} \perp \eta_l \geq 0, \forall l \in L \tag{A.7}$$

$$0 \leq \xi_{x,ai} \perp x_{ai} \geq 0, \forall a \in A; i \in Z \tag{A.8}$$

flow and demand conservation constraints (3), (32), and (55) where H_{ij}, C_{ij}, and ϑ_{ij} are the Lagrangian multipliers associated with Eqs.

(3), (32), and (55). $\xi_{q,l}$, $\xi_{\eta,l}$, and $\xi_{x,ai}$ are the Lagrangian multipliers associated with non-negativity constraints (52)-(54).

If a section l is used by SAV travelers (i.e., $q_l > 0$), then $\xi_{q,l} = 0$ by complementarity constraint (A.6), and consequently $h_l - H_{ij} = 0$ according to Eq. (A.1). If $q_l = 0$, (A.6) enforces $\xi_{q,l} \geq 0$ and (A.1) implies $h_l - H_{ij} \geq 0$.

If extra waiting time is incurred by SAV travelers on a section l (i.e., $\eta_l > 0$), then $\xi_{\eta,l} = 0$ by complementarity constraint (A.7), and consequently $\kappa\pi_l - q_l - \widetilde{q}_l = 0$ according to Eq. (A.2). If $\eta_l = 0$, (A.7) enforces $\xi_{\eta,l} \geq 0$ and (A.2) implies $\kappa\pi_l - q_l - \widetilde{q}_l \geq 0 \Rightarrow q_l + \widetilde{q}_l \leq \kappa\pi_l$.

For HVs, we sum Eq. (A.3) over all links on a route r to obtain $\sum_{a\in A} \delta_{ar}(c_a + C_{D(a),i} - C_{O(a),i} - \xi_{x,ai})$. If route r carries HV flow and $\delta_{ar} = 1$, then $x_{ai} > 0$ and consequently $\xi_{x,ai} = 0 \quad (i = D(r))$ by complementarity constraint (A.8). Following (A.3), $\sum_{a\in A} \delta_{ar}(c_a + C_{D(a),i} - C_{O(a),i}) = 0$, which implies $c_a + C_{D(a),i} = C_{O(a),i}$ that if link a carries HV flow from any zone to zone i ($x_{ai} > 0$), then travel cost on the link plus the minimum generalized travel cost from the end of the link $D(a)$ to zone i should equal the minimum generalized travel cost from the beginning of the link $O(a)$ to zone i.

Recalling utility functions (39)-(40), Eqs. (A.4)-(A.5) can be unified as $\frac{1}{\varphi}\ln Q_{ij}^m + U_{ij}^m + \vartheta_{ij} = 0$, or $Q_{ij}^m = exp(-\varphi(U_{ij}^m + \vartheta_{ij})), \ \forall (i,j) \in \Omega; \ m \in M$. Summing Q_{ij}^m's over vehicle types yields $\sum_{m\in M} Q_{ij}^m = exp(-\varphi\vartheta_{ij}) \sum_{m\in M} exp(-\varphi U_{ij}^m)$. Together with demand conservation constraint (55), we obtain $exp(-\varphi\vartheta_{ij}) = Q_{ij} / \sum_{m\in M} exp(-\varphi U_{ij}^m)$. Plugging this back to $Q_{ij}^m = exp(-\varphi(U_{ij}^m + \vartheta_{ij}))$ gives the logit-based market shares. □

Proof of Proposition 4. All terms in P1 are continuous given the continuous approximations in Eqs. (45)-(47). Therefore, there exists a solution to P1, according to Facchinei and Pang (2003). P2 is continuous as well. In addition, Φ is convex as it is composed of linear and non-negativity constraints. Under the above assumption about η, Φ is also compact. Thus, P2 also has at least one solution, according to Facchinei and Pang (2003). □

Appendix 2. Solving VI-MARUE (P2)

To solve the VI problem (P2), we reformulate it as a regular NLP (P5) below using a primal-dual gap function (Aghassi et al., 2006). P5 can be solved efficiently using commercial NLP solvers.

(P5): NLP-MARUE

$$\min_{(\boldsymbol{q},\boldsymbol{\eta},\boldsymbol{x},\boldsymbol{Q},\boldsymbol{H},\boldsymbol{C},\boldsymbol{\vartheta})} \sum_{l\in L}[h_l q_l + (\kappa\pi_l - q_l - \widetilde{q}_l)\eta_l] + \sum_{i\in Z}\sum_{a\in A} c_a x_{ai} + \sum_{(i,j)\in\Omega}\left[\sum_{m=HV}\left(\gamma_1 PT_j + PC_j^m + \frac{1}{\varphi}\ln Q_{ij}^m\right)Q_{ij}^m + \frac{1}{\varphi}\sum_{m=SAV}\ln\left(Q_{ij}^m\right)Q_{ij}^m\right] - \sum_{(i,j)\in\Omega} Q_{ij}\vartheta_{ij}$$

s.t.

Flow and demand conservation constraints (3), (32), and (55)

Non-negativity constraints (52)-(54) definitional constraints of problem (P1)

$$H_{ij} \leq h_l, \forall l \in L_{ij}; (i,j) \in \Omega \tag{A.9}$$

$$0 \leq \kappa\pi_l - q_l - \widetilde{q}_l, \forall l \in L \tag{A.10}$$

$$C_{O(a),i} - C_{D(a),i} \leq c_a, \forall a \in A; i \in Z \tag{A.11}$$

$$-C_{ij} + \vartheta_{ij} \leq \gamma_1 PT_j + PC_j^m + \frac{1}{\varphi}\ln Q_{ij}^m, \forall (i,j) \in \Omega; m = HV \tag{A.12}$$

$$-H_{ij} + \vartheta_{ij} \leq \frac{1}{\varphi}\ln Q_{ij}^m, \forall (i,j) \in \Omega; m = SAV \tag{A.13}$$

The objective function of P5 excluding the last term represents the objective of a primal linear program (LP) resulting from P2. The last term in the objective function is the objective of its dual LP. Thus, the objective function of P5 gives the gap between the primal and the dual solutions, which should become zero at optimality by LP strong duality.

Appendix 3. Construction of sections for SAV travelers

Step 1: Construction of SAV routes. Given a road network consisting of nodes (as vertices), zones (a subset of nodes that generate/attract SAV traveler demand), and links connecting the nodes, up to 30 shortest-distance SAV routes between any two zones are constructed using Yen's k-shortest path algorithm. For each zone pair, the number of routes is up to 30 with the route length constrained to be no more than three times the length of the shortest-distance route.

Step 2: Construction of SAV traveler network. The SAV traveler network consists of zones (as vertices) and edges. For each zone pair, an edge is constructed if the two zones are visited consecutively by at least one SAV route (i.e., without an intermediate zone in between on the route). The length of the edge is the shortest distance traversing the two zones, among all SAV routes that visit the two zones consecutively.

Step 3: Construction of sections for SAV travelers. With zones and edges, we apply again Yen's k-shortest path algorithm to construct sections for SAV travelers of each OD. Each path is composed of a sequence of edges. For each path out of the algorithm, we check if it is traversed by at least one SAV route. If yes, such a shortest path is considered as a section, whose length is the sum of the component edge lengths. Similar to step 1, we construct up to 30 sections with the section length constrained to be no more than three times the length of the shortest-distance section.

References

AAA, 2015. Your Driving Costs: How Much are You Really Paying to Drive. Available at. Http://Exchange.Aaa.Com/Wp-Content/Uploads/2015/04/Your-Driving-Costs-2015.Pdf.

Aghassi, M., Bertsimas, D., Perakis, G., 2006. Solving asymmetric variational inequalities via convex optimization. Oper. Res. Lett. 34, 481–490.

Azevedo, C.L., Marczuk, K., Raveau, S., Soh, H., Adnan, M., Basak, K., Loganathan, H., Deshmunkh, N., Lee, D., Frazzoli, E., 2016. Microsimulation of demand and supply of autonomous mobility on demand. Transport. Res. Rec. 2564, 21–30.

Ban, X., Liu, H.X., Ferris, M.C., Ran, B., 2008. A link-node complementarity model and solution algorithm for dynamic user equilibria with exact flow propagations. Transport. Res. Part B 42, 823–842.

Ban, X.J., Dessouky, M., Pang, J.S., Fan, R., 2019. A general equilibrium model for transportation systems with e-hailing services and flow congestion. Transport. Res. Part B 129, 273–304.

Belloche, S., 2015. On-street parking search time modelling and validation with survey-based data. Transport. Res. Procedia 6, 313–324.

Bizfluent, 2017. How to Depreciate a Taxi Cab. Available at. https://bizfluent.com/how-12071902-depreciate-taxi-cab.html.

Boesch, P.M., Ciari, F., Axhausen, K.W., 2016. Autonomous vehicle fleet sizes required to serve different levels of demand. Transport. Res. Rec. 2542, 111–119.

Bösch, P.M., Becker, F., Becker, H., Axhausen, K.W., 2018. Cost-based analysis of autonomous mobility services. Transp. Policy 64, 76–91.

Chen, X., Di, X., 2021. Ridesharing user equilibrium with nodal matching cost and its implications for congestion tolling and platform pricing. Transport. Res. Part C 129, 103233.

Chen, Z., He, F., Zhang, L., Yin, Y., 2016a. Optimal deployment of autonomous vehicle lanes with endogenous market penetration. Transport. Res. Part C 72, 143–156.

Chen, T.D., Kockelman, K.M., Hanna, J.P., 2016b. Operations of a shared, autonomous, electric vehicle fleet: Implications of vehicle & charging infrastructure decisions. Transport. Res. Part A 94, 243–254.

Chen, Z., He, F., Yin, Y., 2016c. Optimal deployment of charging lanes for electric vehicles in transportation networks. Transport. Res. Part B 91, 344–365.

Chen, T.D., Kockelman, K.M., 2016. Management of a shared autonomous electric vehicle fleet. Transport. Res. Rec. 2572, 37–46.

Clayton, W., Paddeu, D., Parkhurst, G., Parkin, J., 2020. Autonomous vehicles: who will use them, and will they share? Transport. Plann. Technol. 43 (4), 343–364.

De Cea, J., Fernández, E., 1993. Transit assignment for congested public transport systems: an equilibrium model. Transport. Sci. 27, 133–147.

Di, X., Ban, X., 2019. A unified equilibrium framework of new shared mobility systems. Transport. Res. Part B 129, 50–78.

Di, X., Liu, H.X., Ban, X., Yang, H, 2017. Ridesharing user equilibrium and its implications for high-occupancy toll lane pricing. Transport. Res. Rec. 2667, 39–50.

Di, X., Ma, R., Liu, H.X., Ban, X., 2018. A link-node reformulation of ridesharing user equilibrium with network design. Transport. Res. Part B 112, 230–255.

Fagnant, D.J., Kockelman, K.M., Bansal, P., 2015. Operations of shared autonomous vehicle fleet for Austin, Texas, market. Transport. Res. Rec. 2536, 98–106.

Facchinei, F., Pang, J., 2003. Finite-Dimensional Variational Inequalities and Complementarity Problems, Volume I. Springer.

Fagnant, D.J., Kockelman, K.M., 2018. Dynamic ride-sharing and fleet sizing for a system of shared autonomous vehicles in Austin, Texas. Transportation 45, 143–158.

Fagnant, D.J., Kockelman, K.M., 2014. The travel and environmental implications of shared autonomous vehicles, using agent-based model scenarios. Transport. Res. Part C 40, 1–13.

Farhan, J., Chen, T.D., 2018. Impact of ridesharing on operational efficiency of shared autonomous electric vehicle fleet. Transport. Res. Part C 93, 310–321.

He, F., Yin, Y., Lawphongpanich, S., 2014. Network equilibrium models with battery electric vehicles. Transport. Res. Part B 67, 306–319.

He, F., Shen, Z.M., 2015. Modeling taxi services with smartphone-based e-hailing applications. Transport. Res. Part C 58, 93–106.

Hyland, M., Mahmassani, H.S., 2018. Dynamic autonomous vehicle fleet operations: optimization-based strategies to assign AVs to immediate traveler demand requests. Transport. Res. Part C 92, 278–297.

Indeed, 2021. How Much Does a Taxi Driver Make in the United States. Available at. https://www.indeed.com/career/taxi-driver/salaries.

Jiang, N., Xie, C., Duthie, J.C., Waller, T., 2014. A network equilibrium analysis on destination, route and parking choices with mixed gasoline and electric vehicular flows. EURO J. Transport. Logist. 3, 55–92.

Lam, W.H.K., Li, Z., Huang, H., Wong, S.C., 2006. Modeling time-dependent travel choice problems in road networks with multiple user classes and multiple parking facilities. Transport. Res. Part B 40, 368–395.

Larsson, T., Patriksson, M., 1999. Side constrained traffic equilibrium models— analysis, computation and applications. Transport. Res. Part B 33, 233–264.

Lavieri, P.S., Bhat, C.R., 2019. Modeling individuals' willingness to share trips with strangers in an autonomous vehicle future. Transport. Res. Part A 124, 242–261.

Lawphongpanich, S., Yin, Y., 2010. Solving the Pareto-improving toll problem via manifold suboptimization. Transport. Res. Part C 18, 234–246.

Levin, M.W., 2017. Congestion-aware system optimal route choice for shared autonomous vehicles. Transport. Res. Part C 82, 229–247.

Levin, M.W., Boyles, S.D., 2015. Effects of autonomous vehicle ownership on trip, mode, and route choice. Transport. Res. Rec. 2493, 29–38.

Levin, M.W., Kockelman, K.M., Boyles, S.D., Li, T., 2017. A general framework for modeling shared autonomous vehicles with dynamic network-loading and dynamic ride-sharing application. Comput. Environ. Urban Syst. 64, 373–383.

Li, M., Di, X., Liu, H.X., Huang, H., 2020a. A restricted path-based ridesharing user equilibrium. J. Intell. Transport. Syst. 24 (4), 383–403.

Li, Y., Liu, Y., Xie, J., 2020b. A path-based equilibrium model for ridesharing matching. Transport. Res. Part B 138, 373–405.

Liang, X., Correia, G.H.A., van Arem, B., 2016. Optimizing the service area and trip selection of an electric automated taxi system used for the last mile of train trips. Transport. Res. Part E 93, 115–129.

Liu, Y., Li, Y., 2017. Pricing scheme design of ridesharing program in morning commute problem. Transport. Res. Part C 79, 156–177.

Ma, J., Li, X., Zhou, F., Hao, W., 2017. Designing optimal autonomous vehicle sharing and reservation systems: a linear programming approach. Transport. Res. Part C 84, 124–141.

Ma, J., Xu, M., Meng, Q., Cheng, L., 2020. Ridesharing user equilibrium problem under OD-based surge pricing strategy. Transport. Res. Part B 134, 1–24.

Merfeld, K., Wilhelms, M.P., Henkel, S., Kreutzer, K., 2019. Carsharing with shared autonomous vehicles: uncovering drivers, barriers and future developments–a four-stage Delphi study. Technol. Forecast. Soc. Change 144, 66–81.

Nazari, F., Noruzoliaee, M., Mohammadian, A., 2018. Shared versus private mobility: modeling public interest in autonomous vehicles accounting for latent attitudes. Transport. Res. Part C 97, 456–477.

Noruzoliaee, M., 2018. Supply-demand Equilibrium of Private and Shared Mobility in a Mixed Autonomous/Human Driving Environment. University of Illinois at Chicago. Ph.D. Dissertation.

Noruzoliaee, M., Zou, B., Liu, Y., 2018. Roads in transition: integrated modeling of a manufacturer-traveler-infrastructure system in a mixed autonomous/human driving environment. Transport. Res. Part C 90, 307–333.

Nowakowski, C., Shladover, S.E., Cody, D., Bu, F., O'Connell, J., Spring, J., Dickey, S., Nelson, D, 2010. Cooperative Adaptive Cruise Control: Testing Drivers' Choices of Following Distances. California PATH Program, Institute of Transportation Studies, University of California at Berkeley.

Petrongolo, B., Pissarides, C.A., 2001. Looking into the black box: a survey of the matching function. J. Econ. Lit. 39, 390–431.
Steck, F., Kolarova, V., Bahamonde-Birke, F., Trommer, S., Lenz, B., 2018. How autonomous driving may affect the value of travel time savings for commuting. Transp. Res. Rec., 0361198118757980
Szeto, W.Y., Jiang, Y., 2014. Transit assignment: approach-based formulation, extragradient method, and paradox. Transport. Res. Part B 62, 51–76.
Talebpour, A., Mahmassani, H.S., 2016. Influence of connected and autonomous vehicles on traffic flow stability and throughput. Transport. Res. Part C 71, 143–163.
Train, K.E., 2003. Discrete Choice Methods With Simulation. Cambridge University Press.
Transportation Test Networks. (2017) https://github.com/bstabler/TransportationNetworks.
US DOT, 2016. Revised Departmental Guidance on Valuation of Travel Time in Economic Analysis.
van den Berg, V.A.C., Verhoef, E.T., 2016. Autonomous cars and dynamic bottleneck congestion: the effects on capacity, value of time and preference heterogeneity. Transport. Res. Part B 94, 43–60.
Wang, X., He, F., Yang, H., Oliver Gao, H., 2016. Pricing strategies for a taxi-hailing platform. Transport. Res. Part E 93, 212–231.
Wardrop, J.G., 1952. Some theoretical aspects of road traffic research. Proc. Inst. Civil Eng. 1, 325–362.
Xu, H., Ordóñez, F., Dessouky, M., 2015a. A traffic assignment model for a ridesharing transportation market. J. Adv. Transport. 49, 793–816.
Xu, H., Pang, J., Ordóñez, F., Dessouky, M., 2015b. Complementarity models for traffic equilibrium with ridesharing. Transport. Res. Part B 81, 161–182.
Xu, Z., Yin, Y., Zha, L., 2017. Optimal parking provision for ride-sourcing services. Transport. Res. Part B 105, 559–578.
Yang, H., Leung, C.W.Y., Wong, S.C., Bell, M.G.H., 2010. Equilibria of bilateral taxi–customer searching and meeting on networks. Transport. Res. Part B 44, 1067–1083.
Yang, H., Yang, T., 2011. Equilibrium properties of taxi markets with search frictions. Transport. Res. Part B 45, 696–713.
Yen, J.Y., 1971. Finding the k shortest loopless paths in a network. Manage. Sci. 17, 712–716.
Zha, L., Yin, Y., Yang, H, 2016. Economic analysis of ride-sourcing markets. Transport. Res. Part C 71, 249–266.